





# Inferring Advective Timescales and Overturning Pathways of the Deep Western Boundary Current in the North Atlantic Through Labrador Sea Water Advection

Leah N. Chomiak<sup>1,2,3</sup> , Igor Yashayaev<sup>4</sup>, Denis L. Volkov<sup>2,3</sup> , Claudia Schmid<sup>3</sup> , and James A. Hooper<sup>2,3</sup> 

<sup>1</sup>Rosenstiel School of Marine, Atmospheric, and Earth Science, University of Miami, Miami, FL, USA, <sup>2</sup>Cooperative Institute for Marine and Atmospheric Studies, University of Miami, Miami, FL, USA, <sup>3</sup>Atlantic Oceanographic and Meteorological Laboratory, National Oceanic and Atmospheric Administration, Miami, FL, USA, <sup>4</sup>Bedford Institute of Oceanography, Fisheries and Oceans Canada, Dartmouth, NS, Canada

## Key Points:

- Advection timescales of the Deep Western Boundary Current (DWBC) are inferred from Labrador Sea Water (LSW) convective minima in the North Atlantic
- The two LSW classes examined are observed to advect on different timescales, likely due to varying advective pathways
- An alternative interior-advective pathway observed as a bifurcation in the DWBC advects water to the interior

## Supporting Information:

Supporting Information may be found in the online version of this article.

## Correspondence to:

L. N. Chomiak,  
[leah.chomiak@rsmas.miami.edu](mailto:leah.chomiak@rsmas.miami.edu)

## Citation:

Chomiak, L. N., Yashayaev, I., Volkov, D. L., Schmid, C., & Hooper, J. A. (2022). Inferring advective timescales and overturning pathways of the Deep Western Boundary Current in the North Atlantic through Labrador Sea Water advection. *Journal of Geophysical Research: Oceans*, 127, e2022JC018892. <https://doi.org/10.1029/2022JC018892>

Received 25 MAY 2022

Accepted 11 NOV 2022

## Author Contributions:

**Conceptualization:** Leah N. Chomiak, Igor Yashayaev, Denis L. Volkov

**Data curation:** Leah N. Chomiak, Igor Yashayaev, Claudia Schmid, James A. Hooper

**Formal analysis:** Leah N. Chomiak

**Funding acquisition:** Denis L. Volkov

**Investigation:** Leah N. Chomiak

**Methodology:** Igor Yashayaev, Denis L. Volkov

**Project Administration:** Denis L. Volkov

© 2022. The Authors.

This is an open access article under the terms of the [Creative Commons Attribution License](https://creativecommons.org/licenses/by/4.0/), which permits use, distribution and reproduction in any medium, provided the original work is properly cited.

**Abstract** The Subpolar North Atlantic plays a critical role in the formation of the deep water masses which drive Atlantic Meridional Overturning Circulation (AMOC). Labrador Sea Water (LSW) is formed in the Labrador Sea and exported predominantly via the Deep Western Boundary Current (DWBC). The DWBC is an essential component of the AMOC advecting deep waters southward, flowing at depth along the continental slope of the western Atlantic. By combining sustained hydrographic observations from the Labrador Sea to 26.5°N, we investigate the signal propagation and advective timescales of LSW via the DWBC from its source region to the Tropical Atlantic through various approaches using robust neutral density classifications. Two individually defined LSW classes are observed to advect on timescales that support a new plausible hydrographically observed advective pathway. We find each LSW class to advect on independent timescales, and validate a hypothesized alternative-interior advection pathway branching from the DWBC by observing the arrival of LSW outside of the DWBC in the Bermuda basin on timescales similar to arriving at 26.5°N, 10–15 yr after leaving the source region. Advective timescales estimated herein indicate that this interior pathway is likely the main advective pathway; it remains uncertain whether a direct pathway plays a significant advective role. Using LSW convective signals as advective tracers along the DWBC permits the estimation of advective timescales from the subpolar to tropical latitudes, illuminating deep water advection pathways across the North Atlantic and the lower-limb of AMOC as a whole.

**Plain Language Summary** The Deep Western Boundary Current (DWBC) exports cold and dense deep waters formed in the Subpolar North Atlantic to the tropics, and therefore plays a primary role in global ocean circulation and heat balance. We focus here on Labrador Sea Water (LSW), a water mass formed through wintertime mixing events within the Subpolar North Atlantic characterized by distinctive low-temperature and low-salinity signatures. By following the passage of these signatures through several locations, we investigate the pathways and spreading timescales of LSW from its source region toward the subtropical North Atlantic by the DWBC. We find two distinct LSW masses to reach the same location on independent timescales, and observe LSW in the Central Atlantic just prior to or on the same timescale as being observed in the Tropical Atlantic. These findings indicate that an alternative-interior export pathway branching from the DWBC is likely to exist, exporting LSW away from the continental slope and into the Atlantic interior rather than following a direct equatorward route. Estimating advective timescales and pathways of the DWBC using LSW aid in the present understanding and future prediction of overturning circulation in the Atlantic Ocean.

## 1. Introduction

As the Earth gains and loses heat at low and high latitudes, respectively, the large-scale ocean and atmosphere circulations are characterized by a net poleward heat flux. In the North Atlantic, warm tropical waters are carried northward by a system of wind-driven near-surface currents, dominated by the Gulf Stream and North Atlantic Current. Upon losing heat to the atmosphere en route, these waters become denser and sink in the Subpolar North Atlantic forming North Atlantic Deep Water (NADW) consisting of Labrador Sea Water (LSW), Iceland-Scotland Overflow Water (ISOW), and Denmark Strait Overflow Water (DSOW). These cold and dense waters are collectively exported southward at depths below 1,000 m, constituting the lower limb of the Atlantic

**Resources:** Leah N. Chomiak, Igor Yashayaev, Denis L. Volkov, James A. Hooper  
**Software:** James A. Hooper  
**Supervision:** Igor Yashayaev, Denis L. Volkov  
**Visualization:** Leah N. Chomiak  
**Writing – original draft:** Leah N. Chomiak, Denis L. Volkov  
**Writing – review & editing:** Leah N. Chomiak, Igor Yashayaev, Denis L. Volkov, Claudia Schmid

Meridional Overturning Circulation (AMOC). The exact pathways and time scales of the southward spreading components of NADW are not yet fully understood.

In this study, we focus on the upper component of NADW, dominated by LSW. LSW is formed in the Labrador Sea through wintertime convection. A combination of changes in air-sea heat and freshwater fluxes, local and regional wind patterns, Arctic inflow, continental run-off, advection of heat and salt by the Subpolar North Atlantic circulation, and preconditioning from prior convective events in the Labrador Sea dictate the intensity, depth, volume, and resulting classification of newly formed LSW masses (J. Lazier et al., 2002; Straneo, 2006; Yashayaev, 2007; Yashayaev et al., 2015). Many studies have cataloged the multiyear and decadal trends in the convective formation of LSW in the Labrador Sea (J. Lazier et al., 2002; Straneo, 2006; Yashayaev, 2007; Yashayaev & Loder, 2008, 2016, 2017; van Aken et al., 2011) noting extreme formation events in the late 1970s, 1980s into mid-1990s, early 2000s, and most recently in the latter half of the 2010s, each producing LSW masses identifiable through distinct low-temperature, low-salinity, and high-density signatures. Preconditioning and the resulting characteristics of each developing class have been linked to large-scale changes in the Subpolar North Atlantic, such as a drastic freshening throughout all basins from the 1960s to late 1990s and recently in the 2010s (Dickson et al., 2002; Holliday et al., 2020; Yashayaev, 2007) in addition to a dramatic freshwater influx in the late 2010s possibly related to accelerated melting of the Greenland ice sheet (Dukhovskoy et al., 2019; Yashayaev et al., 2015). Localized mesoscale eddies, such as Irminger Rings spawned from the West Greenland Current, may also play a role in the transport of heat, salt, and freshwater and in Labrador Sea restratification (Chanut et al., 2008; Rieck et al., 2019). Prior studies have called into question the role of the Irminger Basin on the preconditioning and/or formation of LSW (Fröb et al., 2016; Pickart & Spall, 2007; Pickart et al., 2003; Våge et al., 2011; Yashayaev, Bersch, & van Aken, 2007). Convection in the Irminger Basin has been shown to be shallower than in the Labrador Sea, producing convective water masses that are significantly warmer, saltier, and less dense than the LSW counterparts (Yashayaev, Bersch, et al., 2007; Yashayaev & Loder, 2009). Despite the difference in convective processes and mixed layer properties in the Irminger Sea to that of the Labrador Sea, the water convectively mixed in the Irminger Sea in the winter is often also referred to as LSW. Some of this water flows into the Labrador Sea where it can get entrained in the convective formation of true LSW, which is deeper, colder, fresher, and denser than the convectively formed waters in the Irminger Sea. Because of that connection, the Irminger Sea and the convective regions surrounding southern Greenland (Fröb et al., 2016) can be seen as important sources for convective preconditioning in the Labrador Sea. However, the leading driver of deep mixing and formation of LSW in the Labrador Sea is attributed to the cumulative surface heat loss during winter. Fröb et al. (2016) revealed a unique linkage between convective processes occurring over a broad region from the central Labrador Sea to their transition into the Irminger Sea south of Greenland in the winter of 2015, leading to the formation of another voluminous LSW class. However, such broad spatial extent of persistent extreme atmospheric cooling is atypical, and this connection in southern Greenland to the formation of LSW in 2015 has not been supported in years outside of 2015. The LSW class formed through the late 1980s to mid-1990s was shown to be isolated from the winter mixed layer formed in the Irminger Sea, which was saltier and less dense than any LSW of that period (Yashayaev, Bersch, et al., 2007; Figure 2). Similarly, Yashayaev and Loder (2009), using year-round observations from Argo floats in the Subpolar Region, showed that the cold and dense LSW class of 2000 was never connected to the warmer and lighter local mixed layer in the Irminger Sea, and connections between other LSW convective classes and an Irminger influence are not well supported.

Isopycnally constrained thinning of each newly formed LSW mass is evident in temperature, salinity, and density space over time as witnessed through profiling floats and yearly hydrographic occupations in the Labrador Sea on both seasonal and interannual time scales (Yashayaev & Loder, 2016, 2017). A reduction in the volume of the convectively formed LSW mass with time suggests that LSW is subsequently exported out of the basin with its void filled by warmer and saltier water masses, likely of central and eastern Subpolar North Atlantic origin given the influence of the North Atlantic Current. LSW is observed to advect out of the Labrador Sea and spread along various known separate pathways: circulating into the Subpolar North Atlantic (Kieke et al., 2016; Straneo et al., 2003; Yashayaev, Bersch, et al., 2007; Yashayaev & Clarke, 2008; Yashayaev et al., 2015; Yashayaev, van Aken, Holliday, & Bersch, 2007), entraining into the deep layers of the North Atlantic Current system and Central Atlantic (Biló & Johns, 2019; Bower et al., 2011; Straneo et al., 2003), and advecting equatorward out of the Subpolar North Atlantic via the Deep Western Boundary Current (DWBC; Andres et al., 2018; Bower et al., 2011; Handmann et al., 2018; McCartney, 1992; Stramma et al., 2004; Straneo et al., 2003; Zantopp et al., 2017).

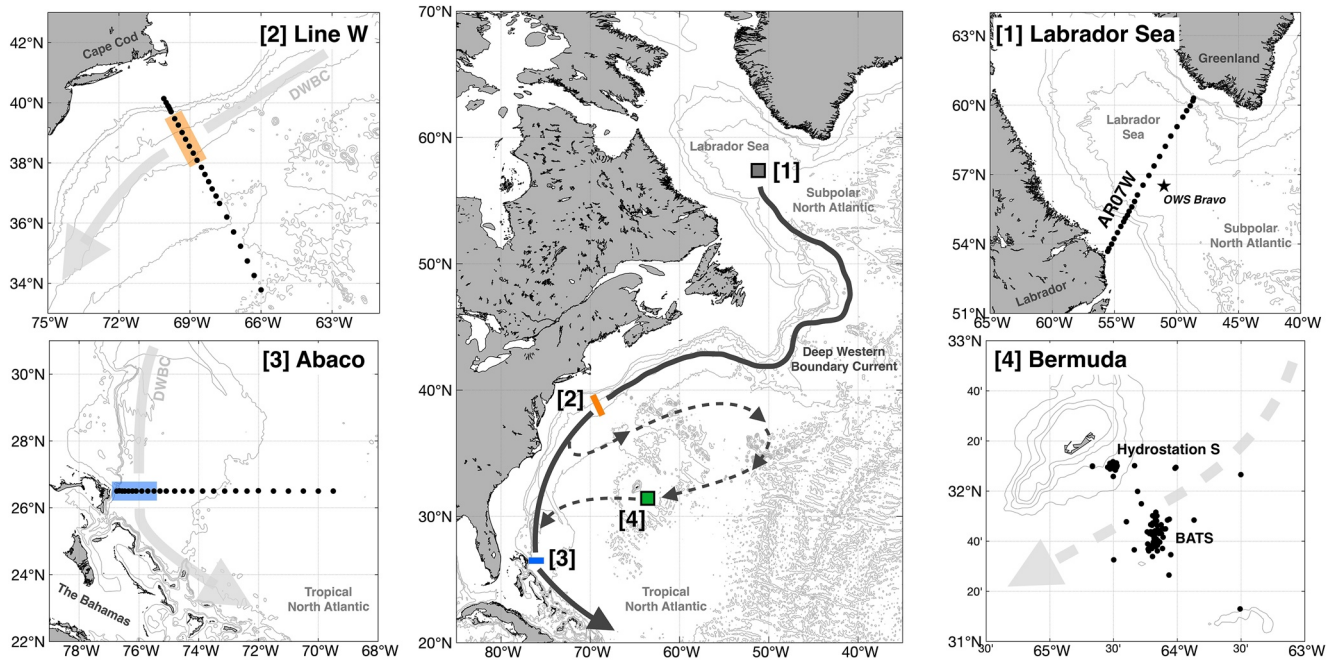


**Figure 1.** Schematic of the four hydrographic locations used in this study (center) and respective station maps: [1] averaged profiles from the central Labrador Sea derived from the WOCE/CLIVAR AR07W line, Ocean Weather Station (OWS) *Bravo*, and Argo at approximately 57°N; [2] WHOI Line W hydrographic line located at 39°N; [3] NOAA WBTS/26.5°N hydrographic line (hereinafter referred to as Abaco) located at 26.5°N; [4] BIOS Bermuda Atlantic Time Series (BATS) Program and Hydrostation S (hereinafter referred to as Bermuda) located at 32°N. Line W and Abaco hydrographic lines intersect the pathway of the Deep Western Boundary Current (DWBC) and only stations within this throughflow are used in this study (orange and blue shaded region, respectively). The idealized, classically understood pathway of the DWBC is approximated by the solid arrow, while the hypothesized alternative advective pathway into the Central Atlantic (adapted from Biló & Johns, 2019) is approximated by the dashed arrow. Bathymetry contours are shown in 1,000 m intervals.

While multiple export pathways of LSW and NADW as a whole are possible (Bower et al., 2019, 2011, 2009; Gary et al., 2012, 2011; Schott et al., 2004; Zou & Lozier, 2016), we focus here solely on the advection of LSW by the DWBC. The DWBC is a southward flowing current along the western continental shelf of the Atlantic Ocean (Figure 1, center) that is responsible for advecting a majority of the newly formed NADW out of the Subpolar North Atlantic. Recent efforts have assessed the variability and transport of the DWBC through use of repeat hydrography and mooring lines at various latitudes spanning the North Atlantic western continental slope (Andres et al., 2018; Cunningham et al., 2007; Johns et al., 2008, 2011; Kanzow et al., 2007; Le Bras et al., 2017; Meinen et al., 2004, 2006; Peña-Molino et al., 2011, 2012; Toole et al., 2011; van Sebille et al., 2011; Zantopp et al., 2017). These and prior efforts have showcased variability in the DWBC as a slowing or even temporary reversal in transport (Johns et al., 2008), offshore meandering away from the continental shelf (Andres et al., 2018; Bower & Hunt, 2000b; Bryden et al., 2005; Spall, 1996a), theorized recirculation patterns in the North Atlantic (Biló & Johns, 2019; Bower & Hunt, 2000a; Spall, 1996b), and localized changes to the source regions of the transported NADW in the Subpolar North Atlantic (Lozier et al., 2019; Petit et al., 2020; Yashayaev, 2007; Yashayaev & Loder, 2016, 2017) perhaps in correlation with the North Atlantic Oscillation (Blaker et al., 2015; Zantopp et al., 2017).

LSW influences many regions of the North Atlantic and is easily identified through its cold, fresh, dense signature, as well as its anomalously low potential vorticity and high concentration of anthropogenic gaseous tracers such as CFCs, CO<sub>2</sub>, and dissolved oxygen (Cunningham & Haine, 1995; Fine et al., 2002; Pickart et al., 2003; Smethie et al., 2000; Talley & McCartney, 1982; Yashayaev, 2007). Numerous studies have observed LSW advection through hydrographic and mooring sections along the DWBC throughout the North Atlantic, noting changes in the physical properties of LSW over time and quantifying advective timescales based on arrival and passage of the source-region convective signal. By following the progression of LSW convective signals along the DWBC, advective timescales of DWBC transport, and consequently the lower-limb of AMOC, can be estimated.

Fine et al. (2002) suggested a 20 yr advective timescale of LSW from the source region to the equator estimated via CFC tracers. Le Bras et al. (2017) found a 3–7 yr lag on the arrival of LSW within the DWBC southeast of

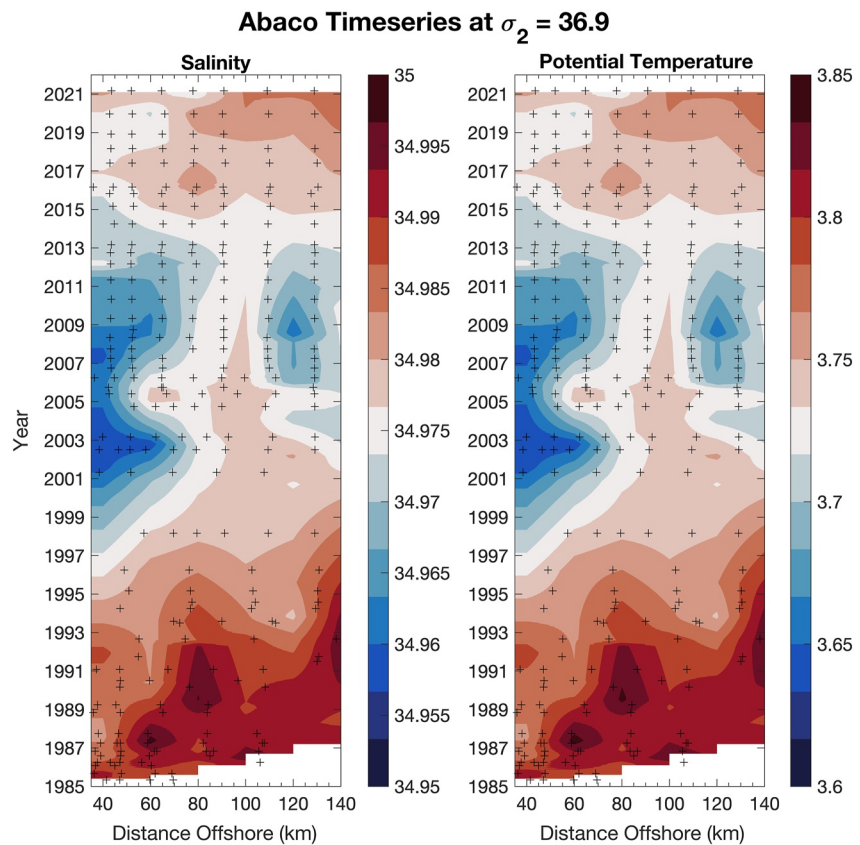


**Figure 2.** Distance-Time diagram showing salinity (PSU, left) and potential temperature ( $^{\circ}\text{C}$ , right) of the Abaco  $26.5^{\circ}\text{N}$  hydrographic section within 140 km off Abaco Island along the predefined  $\sigma_2 = 36.9 \text{ kg/m}^3$  isopycnal, representing the core of Classical LSW (cLSW) within the Deep Western Boundary Current (DWBC) as described by van Sebille et al. (2011) (comparable to Figure 2 of their study). Station occupations are indicated by crosses. This study incorporates the latest decade (since 2011) of observations to the Abaco time series.

Cape Cod along Line W through temperature, salinity, and potential vorticity anomalies (location 2 in Figure 1). Studies assessing DWBC advection of LSW from the source region to Abaco, Bahamas ( $26.5^{\circ}\text{N}$  hydrographic line; location 3 in Figure 1) estimated an advective timescale of 10 yr based on salinity anomalies (Molinari et al., 1998; van Sebille et al., 2011), yet 4 yr based solely on a general circulation model output (van Sebille et al., 2011). Similar efforts had previously looked at the arrival of LSW in the central Atlantic near Bermuda outside of the idealized DWBC pathway (location 4 in Figure 1) and found advective timescales of 6 yr from temperature anomalies (Curry & McCartney, 1996; Curry et al., 1998).

The previous advective assessments from Abaco documented an abrupt onset of a cold, low-salinity signal within the spatially defined classical-LSW (cLSW) layer beginning in the late 1990s (Molinari et al., 1998; van Sebille et al., 2011, see their Figure 2) thought to be in connection to an extreme convective event upstream from the Labrador Sea. The duration of the Abaco time series used in previous studies was, however, insufficient to map the full passage of the signal through this location, as recovery from this cold and fresh state was not yet observed. Presently, with an additional decade of hydrographic surveys at  $26.5^{\circ}\text{N}$  we observe for the first time the complete passage of the convective signal and the onset, or return, of warmer and saltier conditions (Figure 2, comparable to Figure 2 in van Sebille et al., 2011). Looking specifically along the pre-defined cLSW core isopycnal layer at  $\sigma_2 = 36.9 \text{ kg/m}^3$  to compare with previous studies (see van Sebille et al., 2011), the colder and fresher signal is observed to appear first off the coast ( $<80 \text{ km}$ ) of Abaco Island with an abrupt onset in 1997 followed by a rebound to ambient conditions beginning in 2015. A second relatively cold and low-salinity signal is observed further offshore ( $>100 \text{ km}$ ) spanning 2003–2014. Both signals are captured within the DWBC throughflow of the  $26.5^{\circ}\text{N}$  hydrographic line (40–140 km offshore, east of Abaco Island). The complete passage of the convective signal and extended hydrographic observations at  $26.5^{\circ}\text{N}$  serve as the motivation for this study, where we must

look further upstream to investigate both the source and propagation of these signals and their advective timescales in relation to the DWBC.

Past studies (Fine et al., 2002; Le Bras et al., 2017; Molinari et al., 1998; Toole et al., 2011; van Sebille et al., 2011) have classified and partitioned LSW in a variety of ways that challenge the fidelity of such advective time scale estimates, as differing density or depth classifications could likely result in different advective spreading outcomes and may not always reflect the spreading of a water mass class formed explicitly in the Labrador Sea. Different classifications capture different layers containing waters from different sources and different mixing and transformation histories. Differing defining characteristics aside, these previous definitions of LSW also tended to favor local conditions and are thus ill-suited for large-scale assessments of the water mass properties. To combat this issue, we first reclassify LSW through a spatially and temporally all-encompassing approach in a neutral density framework, restructuring previous LSW definitions for one cohesive classification that constrains all previously observed LSW classes within and holds across the vast geographical North Atlantic DWBC domain from the Labrador Sea to the subtropical North Atlantic at 26.5°N. We utilize LSW vintage-class classification (e.g., LSW<sub>1987–1994</sub>) structured by Yashayaev (2007), rather than solely defining LSW in static vertical layers such as the upper-LSW (uLSW), classical-LSW (cLSW), and deep-LSW (dLSW) classifications commonly used in models and previous assessments of LSW (e.g., Biló & Johns, 2019; Le Bras et al., 2017; Molinari et al., 1998; Toole et al., 2011; van Sebille et al., 2011). We then assess the advection of LSW using a compilation of updated hydrographic time series at two locations along the North American continental shelf and incorporate hydrographic data from the Bermuda basin in the Central Atlantic as a counter-location outside of the classically understood DWBC advective pathway (Figure 1). Recent studies have showcased recirculation of LSW into the Central Atlantic (see Biló & Johns, 2019), and others have debated whether a bifurcation in DWBC advection exists in the Gulf Stream-DWBC crossover region near Cape Hatteras advecting LSW both into the Atlantic interior as well as equatorward along the continental slope (Andres et al., 2018; Bower & Hunt, 2000a, 2000b; Spall, 1996a, 1996b). These hypothesized and proposed recirculation pathways have the potential to alter or delay advective timescales of LSW and subsequent NADW.

Improved estimates of the advective pathways and timescales of NADW are critical to better understand the role of the AMOC in the climate system. Here, by using hydrographic observations at several locations we seek to observe the propagating LSW convective signal and to estimate advective timescales of the DWBC in the North Atlantic. In addition, through the assessment of LSW advective timescales at each hydrographic location, we aim to gain insight into DWBC advective pathways.

## 2. Data and Methods

### 2.1. Hydrographic Data

The propagation of LSW in the North Atlantic is assessed by compiling data from sustained repeat hydrographic surveys in the following four geographic locations (Figure 1): the Labrador Sea (WOCE line AR07W, Ocean Weather Station *Bravo*, and Argo), off the south-east coast of Cape Cod at 39°N (WHOI Line W time series program, hereinafter referred to as Line W), the Bermuda basin at 32°N (BIOS Bermuda Atlantic Time Series [BATS] and Hydrostation S programs), and off the east coast of Abaco Island, Bahamas at 26.5°N (NOAA Western Boundary Time Series program, hereinafter referred to as Abaco). Full-depth hydrographic observations in the Labrador Sea serve as the source region data set for this study, highlighting the unique convective events characteristic to the region, while Line W and Abaco serve as LSW observation checkpoints along the DWBC. The Bermuda basin serves as a counter location outside of the classically understood advective pathway of the DWBC, allowing for investigation of the hypothesized alternative-advective pathway.

A collection of historical data, sustained hydrographic occupations of the trans-basin WOCE/CLIVAR AR07W line, and Argo profiling floats comprise the Labrador Sea data set presented in this study, consisting of five decades made current up to the year 2020 (Yashayaev & Loder, 2016, 2017). Yearly occupations of the AR07W hydrographic line have been conducted by the Bedford Institute of Oceanography (BIO) of Fisheries and Oceans Canada and several other international organizations since 1990 continuing into present day. Prior to 1990, data is supplemented with the US Coast Guard's Ocean Weather Station *Bravo* time series (1964–1974), BIO surveys (1977–1988), and from international surveying partnerships and data centers (Kieke & Yashayaev, 2015; J. R. N. Lazier, 1980; Yashayaev, 2007). Annually averaged vertical profiles of temperature and salinity are constructed

for the central Labrador Sea (see methods in Yashayaev, 2007 and Yashayaev & Loder, 2016), used here in this study spanning the years 1970–2020, with the longest data gap spanning 1978–1981.

Hydrographic data along the Line W transect (39°N) serve as the first observational checkpoint along the DWBC. The Line W hydrographic field program led by Woods Hole Oceanographic Institution (WHOI) was active during the years 1994–2014, supporting repeat hydrographic missions and an installation of six moorings perpendicular to the continental slope off Cape Cod stretching into the Gulf Stream capturing the throughflow of the DWBC along the slope (Toole et al., 2011). A standard cruise track was repeated approximately every year, in some cases twice per year, sampling shelf waters and down the slope into the Gulf Stream. A gap in data collection occurred between the years 1998–2001.

Hydrographic data along the Abaco transect serve as the second observational checkpoint along the DWBC. The transect runs along 26.5°N due east off the coast of Abaco Island, Bahamas with full-depth CTD casts at stations located between  $-76.9^{\circ}\text{W}$  and  $-69^{\circ}\text{W}$ . The Abaco transect has been surveyed quasi-annually since 1985 to present day as part of the NOAA Western Boundary Time Series (WBTS) project, the University of Miami Rosenstiel School of Marine, Atmospheric, and Earth Science's Meridional Overturning Circulation and Heat-flux Array (MOCHA) project, and the National Oceanographic Center's (UK) RAPID program. A multi-year collaboration between these projects has been the backbone of sustained monitoring of the strength of the AMOC at 26.5°N through repeat hydrographic surveys and mooring installations. Data presented in this study range from the beginning of collection in 1985–2021, with a gap in data collection occurring between the years 1998–2001.

Hydrographic data from the Hydrostation S and BATS programs are used to investigate the plausible advective spread of LSW outside of the perceived DWBC pathway and into the central Atlantic basin near Bermuda. The Bermuda Institute of Oceanography Hydrostation S deep-water research mooring located 22 km southeast of Bermuda began collection in 1954 with full-depth ( $>3,000$  m) bi-weekly sampling, followed by the expansion into the BATS program beginning in 1988 conducting monthly deep hydrographic surveys in the Bermuda basin, located 88 km southeast of the Bermuda coast. The Bermuda basin data set presented in this study reflects a cumulated collection of Hydrostation S and BATS hydrographic CTD data spanning the years 1989–2019.

## 2.2. Data Processing

Hydrographic CTD data from the Labrador Sea, Line W, Bermuda, and Abaco time series programs were pre-processed, calibrated and quality controlled via the methods described in BATS Methods (1997), Hooper et al. (2020), Yashayaev (2007), Yashayaev and Loder (2009, 2016), and Toole et al. (2011), respectively.

Hydrographic data at Line W and Abaco locations are geographically constrained to isolate the stations within the DWBC throughflow (Figure 1, orange and blue shading), as identified by Line W mooring data showcasing enhanced velocity and net southward transport in Toole et al. (2011), and similarly for Abaco showcased by mooring data (Biló & Johns, 2020; Johns et al., 2008, 2011) and through previous studies (Molinari et al., 1998; van Sebille et al., 2011). Line W station data are constrained to the geographical limits of  $39.600^{\circ}\text{N}$ ,  $-69.718^{\circ}\text{W}$  and  $38.073^{\circ}\text{N}$ ,  $-68.667^{\circ}\text{W}$  along each transect representing the first and last moorings within this throughflow (w1–w5, Toole et al., 2011). The DWBC throughflow is observed within an approximated 100 km range off the coast of Abaco along  $26.5^{\circ}\text{N}$  (Biló & Johns, 2020; Johns et al., 2008, 2011; Molinari et al., 1992, 1998), and similarly to Line W, station data at Abaco are constrained to the geographical limits of  $-76.9^{\circ}\text{W}$  and  $-75.5^{\circ}\text{W}$  along  $26.5^{\circ}\text{N}$ . All outlying station data outside of the Line W and Abaco transect geographical constraints are omitted from analysis.

A secondary round of processing and quality control is performed to limit the impact of short-term ( $<1$  yr) variability associated with eddies, planetary waves, and/or Gulf Stream or Subtropical Gyre intrusion (detailed further in the Supporting Information, Section S2 in Supporting Information S1). To reduce the influence of surrounding warmer and saltier water masses on the LSW signal, such as Mediterranean Overflow Water (MOW), average potential temperature and salinity values over a wide-spread intermediate depth layer are computed for each station across all data sets downstream of the Labrador Sea. Stations within the defined layer that exceed the designated maximum cutoffs atop of the 25th percentile of values are excluded from analysis (refer to Section S3 in Supporting Information S1 for details). Without the exclusion of MOW from the LSW signal, LSW cores would be warmer and saltier and the passage of each signal skewed by the influence of MOW. The percentage of omitted stations from both phases of secondary cleaning total 13% for the Line W data set, 47% for the Bermuda

data set, and 11% for the Abaco data set. The final number of profiles used for analysis total 45 annually averaged profiles for the Labrador Sea, 130 profiles (24 occupations) for Line W, 657 profiles (31 annually averaged profiles) for Bermuda, and 371 profiles (50 occupations) for Abaco.

Full-depth profiles and hydrographic sections are linearly projected along a uniformly equidistant pressure grid beginning at the surface and are then zonally averaged for each occupation (Line W, Abaco) or each year (Labrador Sea, Bermuda basin). Data sets are not interpolated, and therefore maintain original gaps. Line W and Abaco sections are zonally averaged using a distance-weighted averaging scheme due to the spatial variability in transect sampling, where individual stations are weighted by the relative distance covered over the constrained transect length (refer to Section S4 in Supporting Information S1). For all locations, salinity is reported in practical salinity units (PSU), temperature (T90 scale) is converted to potential temperature referenced to the surface, and potential vorticity (defined as  $q = (f * N^2)/g$  using the Brunt-Vaisala frequency,  $N^2 = (-g/\partial\rho) (\partial\rho/\partial z)$ , where  $f$  is the Coriolis parameter and  $g$  is gravity) is calculated and smoothed with a locally weighted scatterplot smoothing (LOWESS) method. Analyses in the forthcoming Sections 3.2.1, 3.2.2, and 3.2.3 utilize data sets that are monthly interpolated and the original data gaps are maintained.

### 2.3. Defining LSW

Previous studies have defined LSW in a variety of ways: in depth space (Fine & Molinari, 1988), potential density referenced to the surface ( $\sigma_\theta$ ; Kieke et al., 2006; Rhein et al., 2007; Yashayaev, 2007), 1,000 m ( $\sigma_1$ ; Yashayaev, 2007), 1,500 m ( $\sigma_{1.5}$ ; Molinari et al., 1998), and 2,000 m ( $\sigma_2$ ; van Sebille et al., 2011; Yashayaev, 2007), and also in neutral density space ( $\gamma_n$ ; Hall et al., 2004; Le Bras et al., 2017; Toole et al., 2011). LSW has historically been classified in static-spatial layer classifications, such as classical-LSW (cLSW), upper-LSW (uLSW), and deep-LSW (dLSW) (Le Bras et al., 2017; Molinari et al., 1998; Toole et al., 2011; van Sebille et al., 2011), as well as individually through volumetric vintage-class classification (Yashayaev, 2007).

While several classifications exist, each pertain to different eras of data observed and are subject to observer bias. We find these previous definitions to not hold across the geographic locations considered herein. Specifically, the previous classifications fail to constrain all LSW classes where important convective signals are often overlooked in analyses due to the boundaries imposed (showcased in Figure 3), rendering joint ramifications in the case of LSW advection and large-scale AMOC modeling efforts. It is also important to note that while these static-spatial layers define a layer to be “LSW”, the layer may not contain LSW for the entire duration of time, as LSW is produced in convective bursts and advects in patches rather than as a continuous mass. Consequently, over time, the defined layer may contain only patches of LSW surrounded by ambient surrounding water masses.

Taking into consideration the varying nature of LSW formation and properties (e.g., Yashayaev & Loder, 2016, 2017) and improving on the challenges imposed by the previous defining conventions, we introduce a modified reclassification through a spatially and temporally all-encompassing approach in a neutral density framework, restructuring previous LSW-layer definitions for a cohesive classification that holds across the vast geographical North Atlantic DWBC domain from the Labrador Sea to 26.5°N. We first subdivide advected NADW into three layers: Intermediate, Deep, and Abyssal, as defined by neutral density ( $\gamma_n$ , kg/m<sup>3</sup>) constraints that are consistent among all four geographic locations (Figure 3). Neutral density serves as the ideal isopycnal metric to identify LSW across the vast geographical range presented in this study due to the reliance on geographic position factored into its derivation (Jackett & McDougall, 1997). We assume advection along lines of constant neutral density, with little to no diapycnal mixing. However, we find a  $-0.015$  kg/m<sup>3</sup> neutral density shift observed through isolated LSW cores evident at all hydrographic locations outside of the source region (refer to Section S1 in Supporting Information S1). Therefore, a  $+0.015$  kg/m<sup>3</sup> neutral density offset is applied to the Line W, Bermuda, and Abaco data sets to limit the impact of diapycnal mixing.

These constant neutral density isopycnals summarize the ranges of NADW water masses advected out of the Subpolar North Atlantic via the DWBC. The intermediate layer, defined as  $\gamma_n = 27.87$ – $28.01$ , constrains the vast range of LSW classes formed in the Labrador Sea over the past five decades, both locally in the source region as well as at the downstream locations. This range is supported by the minimum in potential vorticity and the potential temperature and salinity minima characteristic to each LSW convective event (Figures 4–6). The deep layer is defined as  $\gamma_n = 28.01$ – $28.10$ , constraining ISOW masses, and the abyssal layer is defined as  $\gamma_n > 28.10$ , constraining DSOW and other dense bottom waters. The defined intermediate layer serves as the primary subset of data

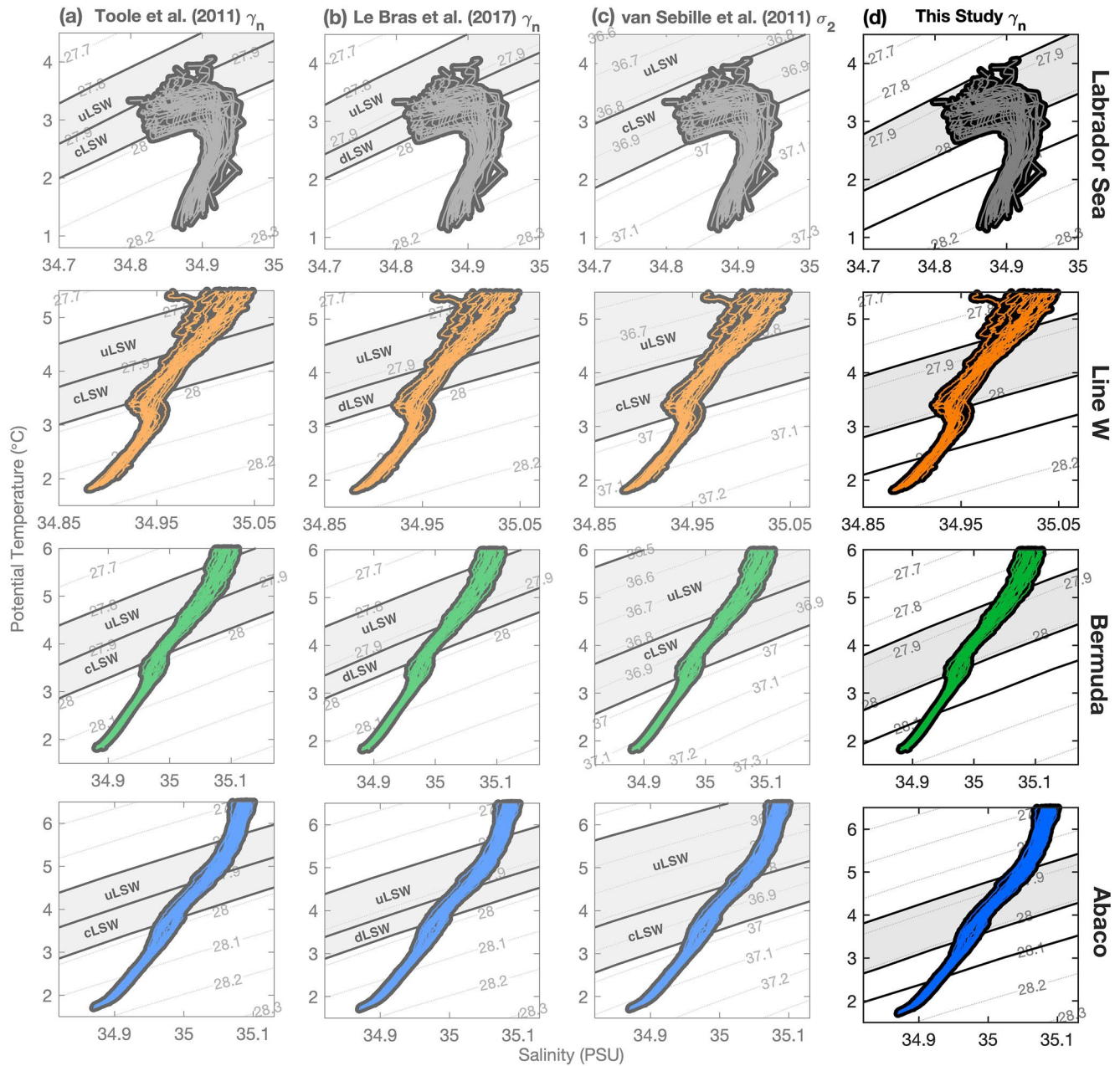


**Figure 3.** Comparative potential temperature-salinity diagrams with density (neutral and sigma-2,  $\text{kg/m}^3$ ) contours of profiles from all four hydrographic locations showcasing various density classifications: (a) neutral density Labrador Sea Water (LSW) definitions of Toole et al. (2011) defined in uLSW and cLSW layers, (b) neutral density LSW definitions of Le Bras et al. (2017) defined in uLSW and dLSW layers, (c) sigma-2 LSW density definitions of van Sebille et al. (2011) defined in uLSW and cLSW layers, and (d) the proposed neutral density layer definitions of this study across all four locations. Uniform neutral density layer definitions proposed in this study (d) are highlighted by the thick black contours: Intermediate (shaded region,  $\gamma_n = 27.87\text{--}28.01$ ), Deep ( $\gamma_n = 28.01\text{--}28.10$ ), and Abyssal ( $\gamma_n > 28.10$ ) layers, where the shaded Intermediate layer constrains all LSW classes characterized within the Labrador Sea time series across all locations. For all panels, Labrador Sea profiles are restricted to  $>300$  m and years 1970–2021, Line W profiles span years 1994–2014, Bermuda profiles span years 1988–2019, and Abaco profiles span years 1985–2021.

presented in this study, as all LSW classes— $\text{LSW}_{1976}$ ,  $\text{LSW}_{1987\text{--}1994}$ ,  $\text{LSW}_{2000\text{--}2003}$ ,  $\text{LSW}_{2012\text{--}2016}$  (Yashayaev, 2007; Yashayaev & Loder, 2017)—can be distinguished and identified based on their unique convective isopycnal imprints within these isopycnal bounds. These definitions, although fixed for the period of study, may need to be revised with time as new LSW classes are formed and new observations are collected.



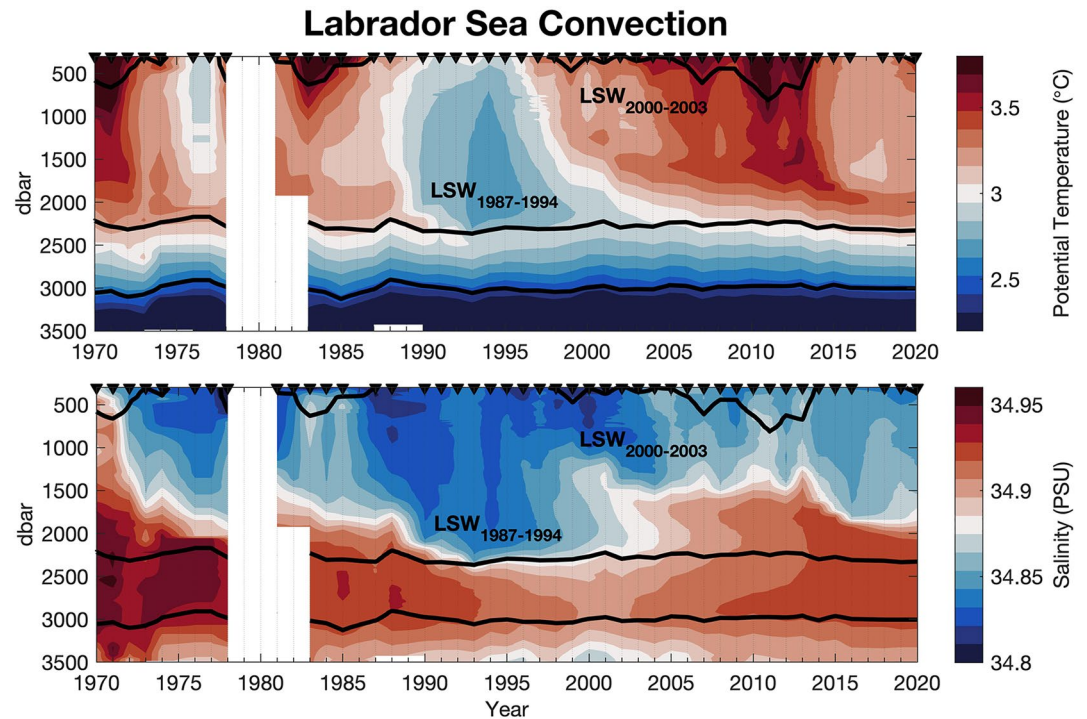


**Figure 4.** Annual isopycnic averages of full-depth potential temperature and salinity profiles in the central region of the Labrador Sea defined by Yashayaev and Loder (2016). Convective events are evident in the late 1970s, mid-1980s–1990s, early 2000s, and mid-2010s to present by the convective imprints of a decrease in temperature and freshening. Contour lines indicate the North Atlantic Deep Water (NADW) layer definitions of this study: intermediate (top,  $\gamma_n = 27.87\text{--}28.01$ ); deep (mid,  $\gamma_n = 28.01\text{--}28.10$ ); abyssal (bottom,  $\gamma_n > 28.10$ ). Yearly averaged profiles are marked by the black triangles.

### 3. Results

#### 3.1. LSW Source Region Properties and Downstream Changes

Convective events in the Labrador Sea in the late 1970s, 1980s to mid-1990s, early 2000s, and most recently in the mid-2010s produced LSW classes distinguishable by anomalously cold, fresh, and dense water (Figure 4; Yashayaev, 2007; Yashayaev & Loder, 2016). In the Labrador Sea, the LSW<sub>1987–1994</sub> convective signal dominates the intermediate layer with the most significant temperature and salinity change in the historical record, with minima in 1994 stretching 2,300 m deep (isopycnal level of  $\gamma_n = 27.99$ ) at 2.7°C and 34.83 PSU, approximately 0.5°C colder and 0.10 PSU fresher than usual. This convective imprint has been subsequently exported out of the basin, observed as both recirculating back into the Subpolar North Atlantic (Yashayaev, Bersch, et al., 2007; Yashayaev, van Aken, et al., 2007) as well as advecting southward into the Atlantic via the DWBC. The signatures of LSW associated with this convective signal are identifiable in all three Atlantic data sets through a minimum in potential vorticity, and anomalous minima in potential temperature and salinity (Figures 5–7). The following convective event, LSW<sub>2000–2003</sub>, reached depths of 1,500 m (isopycnal level of  $\gamma_n = 27.90$ ) with minima in 2000 of 3.15°C and 34.82, rendering it warmer, slightly fresher, and less dense than its more intense predecessor.

As LSW spreads equatorward following the DWBC and/or other possible pathways it thins out and mixes with other water masses, including previously formed recirculating LSW classes. This makes a direct identification of the potential temperature and salinity signals of these specific LSW classes at remote locations downstream often challenging. It should be noted that while we follow the advection of LSW along constant isopycnals, an increase in the potential temperature and salinity of the identified LSW classes (Section 3.2.2, Table 1) and the intermediate layer entirely (see Figure 6) suggest modification or mixing with surrounding intermediate waters along the equatorward advective journey. The greatest change in potential temperature and salinity for both LSW classes (LSW<sub>1987–1994</sub> and LSW<sub>2000–2003</sub>) is observed between the source region (Labrador Sea) and Line W, where LSW drastically warms and becomes more saline on scales of +0.50°C–1.00°C and +0.10–0.15 PSU, respectively (see Table 1 in Section 3.2.2). Further warming and salinification is observed downstream between

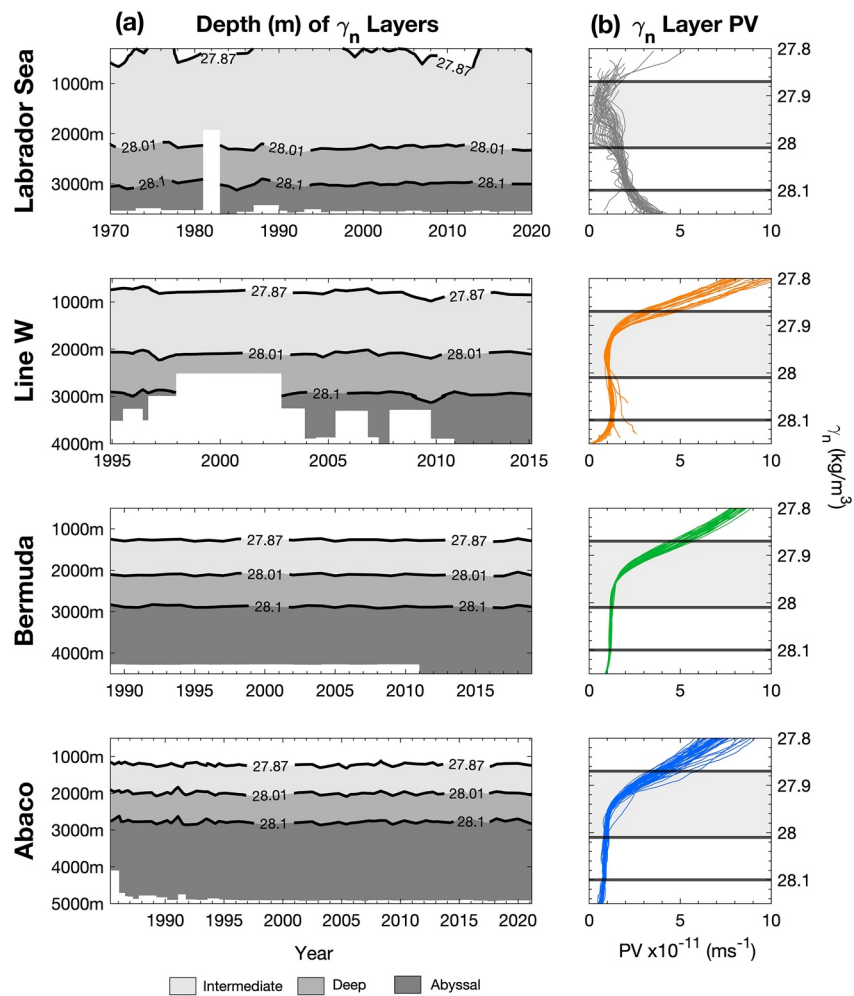


**Figure 5.** Density layer characteristics across all four hydrographic time series showcasing the depth range of each layer (a) and potential vorticity across the defined layers (intermediate, shaded,  $\gamma_n = 27.87\text{--}28.01$ ; deep  $\gamma_n = 28.01\text{--}28.10$ ; abyssal  $\gamma_n > 28.10$ ), where the minimum in potential vorticity is characteristic of Labrador Sea Water (LSW) within the shaded intermediate layer (observed as  $1 \times 10^{-11} \text{ ms}^{-1}$ ).

Line W and Bermuda and Abaco, but with less drastic temperature and salinity changes of  $+0.10^\circ\text{C}\text{--}0.30^\circ\text{C}$  and  $+0.02\text{--}0.05$  PSU, respectively. This further suggests that among the three downstream locations the largest modification of LSW occurs between export out of the Labrador Sea and before arriving at Line W. This could be a result of possible recirculation within the Subpolar North Atlantic and interaction with warmer and saltier North Atlantic Current waters (Yashayaev, Bersch, et al., 2007; Yashayaev, van Aken, et al., 2007) and/or with other surrounding intermediate waters prior to arrival at Line W. Although mixing interactions are not the focus of this study, we can speculate why the property shifts in LSW are observed. MOW occupies a similar density range as LSW, but it is generally warmer and saltier than LSW (van Aken, 2000). Van Sebille et al. (2011), although using a different density range to define LSW, estimated the mixing fraction of MOW with LSW along the Abaco transect to be 20%. The influence of MOW on the observed temperature and salinity convective signals within LSW were deemed to be negligible, therefore, implying that the observed temperature and salinity shifts originated in the LSW source region and were not an outcome of MOW interaction. Because, as mentioned above, the greatest modification to the advected LSW occurs prior to Line W—suggesting a greater subpolar or slope-water influence than Mediterranean influence—it is difficult to judge the impact MOW has on LSW in the western Atlantic. Profiles characteristic of MOW were excluded from data sets and subsequent analyses as described previously in Section 2.2 (refer to Section S3 in Supporting Information S1), and the relevant contributions of MOW at each location are inferred there by the percent of stations removed from each location. For this study, we assume a negligible impact of MOW and other intermediate waters on the

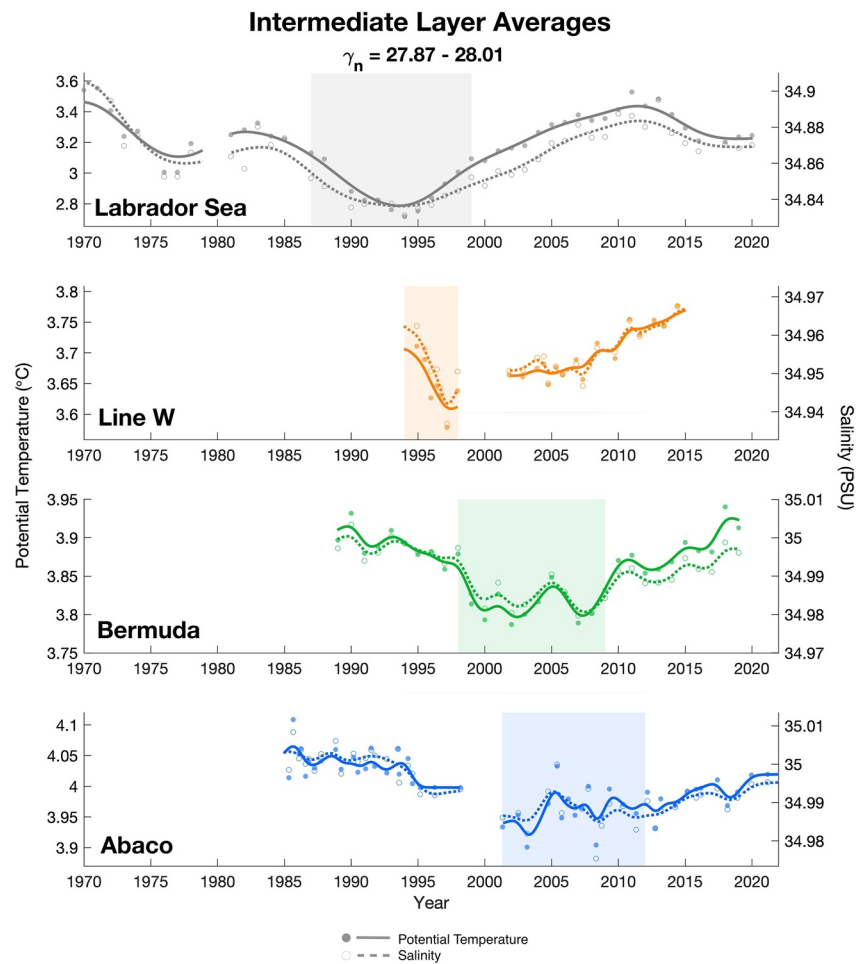


**Figure 6.** Averaged potential temperature (solid line) and salinity (dashed line) of the defined Intermediate layer ( $\gamma_n = 27.87-28.01$ ) for each data set. Curves are shown smoothed and monthly interpolated, while filled (potential temperature) and open (salinity) circles mark individual unsmoothed and uninterpolated data points. Layer averaging indicates minima in 1994 in the Labrador Sea, 1997 at Line W, and dual minima in 2003 (potential temperature, solid) and 2008 (salinity, dashed) at both Bermuda and Abaco. The shaded region represents the approximate evolution of the convective minima defined through visual assessment. Averaging errors are minimal and insignificant and are not displayed in figure, but to summarize: the average standard errors of the entire averaged intermediate layer data sets (standard error of the mean for each marked datapoint, averaged over the entire time series with resulting standard deviations from the mean standard error) are  $0.0024^{\circ}\text{C} \pm 0.0011^{\circ}\text{C}$  and  $0.0005 \pm 0.0002$  PSU for the Labrador Sea,  $0.0147^{\circ}\text{C} \pm 0.0006^{\circ}\text{C}$  and  $0.0006 \pm 0.0001$  PSU for Line W,  $0.0213^{\circ}\text{C} \pm 0.0013^{\circ}\text{C}$  and  $0.0012 \pm 0.0002$  PSU for Bermuda, and  $0.0140^{\circ}\text{C} \pm 0.0010^{\circ}\text{C}$  and  $0.0007 \pm 0.0001$  PSU for Abaco.

observed convective signals within LSW by the discrete removal of the MOW influence on the hydrographic data sets. We further declare that the observed LSW convective signals are directly related to the changes in the source region (Figure 4) and not acquired through a shift in mixing downstream from the source and other interactions within the DWBC. However, we do not dismiss the likely influence of entrainment, mixing, and/or modification of LSW by saltier waters—a caveat which was accounted for and removed by the aforementioned data cleaning scheme. Further investigation is needed to determine the mixing influence of surrounding waters on the advected LSW once it leaves the Labrador Sea. We acknowledge that LSW is modified as it is advected out of the source region, as this is supported by the hydrographic data presented here in this study, however mixing sources and fractions are not the focus of this study and we employ strict data cleaning procedures to reduce this impact to focus solely on advective timescales. Here, we utilize LSW convective signals as advective tracers on both broad and specific scales through the following three approaches to gauge timescale estimates of lower-limb AMOC transport via the DWBC.

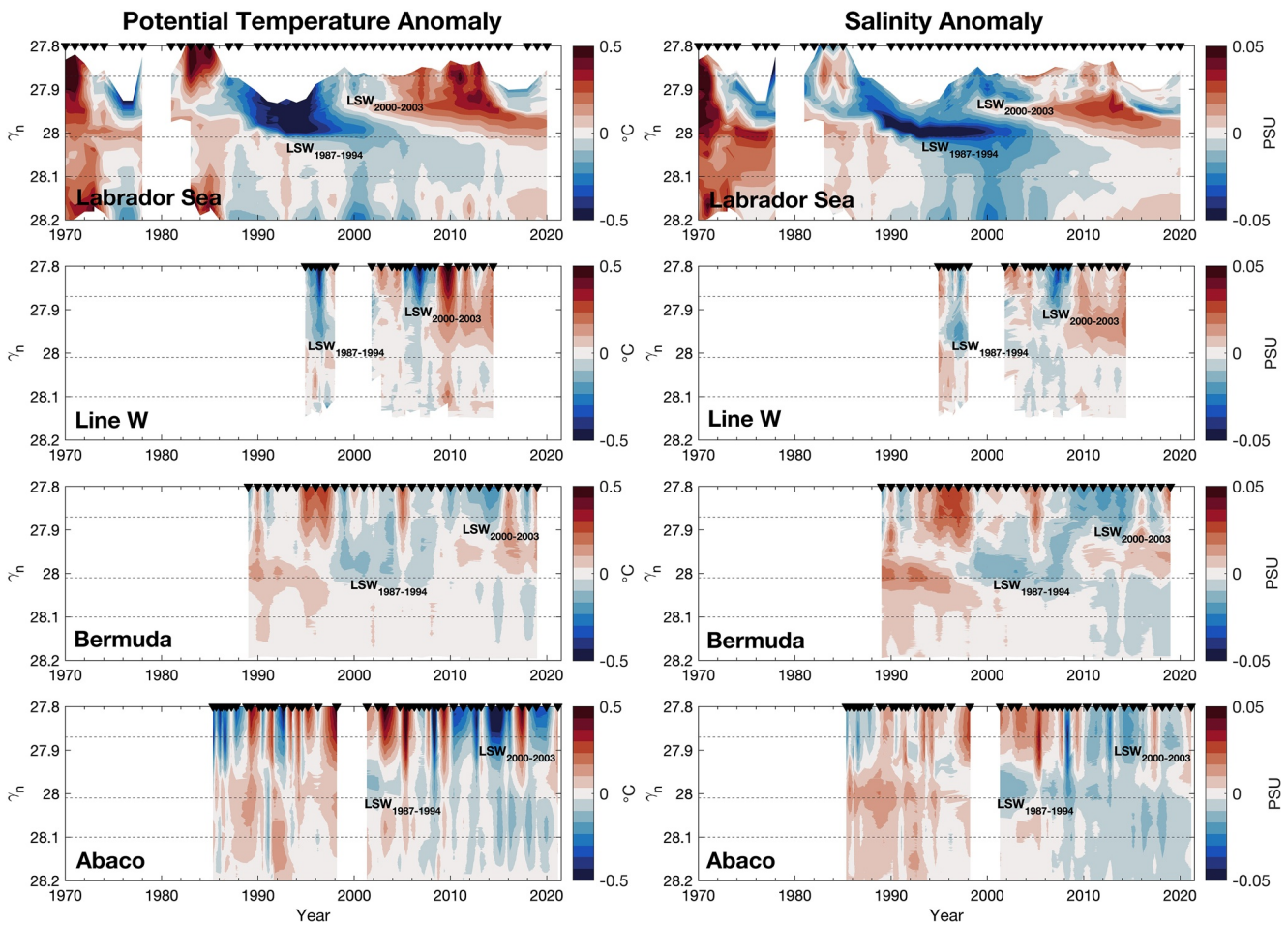


**Figure 7.** Potential temperature (left panels) and salinity (right panels) anomalies of the Labrador Sea (top), Line W, Bermuda, and Abaco (bottom) hydrographic time series in neutral density ( $\gamma_n$ ) space over time. Dashed horizontal lines indicate the isopycnal boundaries between the defined intermediate, deep, and abyssal layers at  $\gamma_n = 27.87, 28.01,$  and  $28.10 \text{ kg/m}^3$ . The two Labrador Sea Water (LSW) masses of interest are indicated below their respective anomalously cold and fresh signals at each location. Hydrographic occupations are indicated by the black triangles at the top of each plot.

**Table 1**

*Potential Temperature and Salinity Minima and Corresponding Year of the Monthly Interpolated LSW<sub>1987–1994</sub> Isopycnal Core  $\gamma_n = 27.99$  (Top) and LSW<sub>2000–2003</sub> Isopycnal Core  $\gamma_n = 27.90$  (Bottom) Across All Locations of Study (See Figure 8), With the Approximated Lag Time in Years From the Labrador Sea Based on the Arrival of the Minima Signals*

| LSW <sub>1987–1994</sub> | Labrador Sea  | Line W        | Bermuda             | Abaco                        |
|--------------------------|---------------|---------------|---------------------|------------------------------|
| °C                       | 2.723 [1994]  | 3.244 [1997]  | 3.358 [2003]        | 3.560 [2003]                 |
| PSU                      | 34.837 [1994] | 34.933 [1997] | 34.954 [2003]       | 34.963 [2003]                |
|                          | +0 yr         | +3 yr         | +9 yr               | +9 yr                        |
| LSW <sub>2000–2003</sub> | Labrador Sea  | Line W        | Bermuda             | Abaco                        |
| °C                       | 3.158 [2000]  | 4.107 [2007]  | 4.411 [2012, 2014]  | 4.504 [2008], 4.527 [2013]   |
| PSU                      | 34.823 [2000] | 34.960 [2007] | 35.014 [2012, 2014] | 35.011 [2008], 35.015 [2011] |
|                          | +0 yr         | +7 yr         | +12–14 yr           | +8, 11–13 yr                 |

### 3.2. Advective Timescales

#### 3.2.1. Intermediate Layer Approach

We first identify the evolution of LSW at all downstream locations through a broad assessment of the defined intermediate layer, following the approach of previous studies (van Sebille et al., 2011, their uLSW and cLSW layer; Le Bras et al., 2017, their uLSW and dLSW layers). LSW, and other advected NADW, can be characterized by a minimum in the potential vorticity, and we use this minimum (approximately  $1 \times 10^{-11} \text{ ms}^{-1}$ ) to support the definition of the intermediate layer (Figure 5). In the Labrador Sea, this intermediate layer covers most of the water column, ranging 500–2,300 m (1,800 m thickness). This isopycnal layer contracts to 800–2,100 m (1,300 m thickness) at Line W, further to 1,300–2,100 m (800 m thickness) in the Bermuda basin and 1,200–2,000 m (800 m thickness) at Abaco, likely due to subduction under the Subtropical Gyre and/or thinning of the layer to conserve potential vorticity (Figure 5).

Potential temperature and salinity of the horizontally averaged data sets are also vertically averaged within the neutral density bounds of the intermediate layer ( $\gamma_n = 27.87\text{--}28.01$ ) to produce a time series of intermediate layer change. Potential vorticity is not used as a tracer because the convective cores cannot be isolated to desired detail in high resolution, as potential vorticity remains nearly uniform over the layer of interest. Potential vorticity is used in the study only as a supporting parameter defining the Intermediate layer and LSW presence; potential temperature and salinity serve as the best advective tracers. Figure 6 showcases the potential temperature (filled circles) and salinity (empty circles) averaged in the intermediate layer with a monthly interpolated, smoothed (a low-pass Gaussian filter with a cutoff period of 1 yr is applied) time series atop across all locations. Like the previous LSW advective estimates of Le Bras et al. (2017), Molinari et al. (1998), and van Sebille et al. (2011), we use the minima in average potential temperature and salinity of our defined intermediate layer to derive advective timescales. The 1994 minima in potential temperature and salinity in the Labrador Sea is observed 3 yr later at Line W in 1997, where an initial drop in temperature and salinity is observed just prior to the 4 yr data gap in the time series, unfortunately. It is unclear whether a further minimum would be observed at Line W had data been collected between 1998 and 2001. Dual minima in 2003 (potential temperature, solid line) and 2008 (salinity, dashed line) are observed to occur almost simultaneously further downstream at both Abaco and Bermuda, giving advective timescales of 9–14 yr based on the arrival of the dual minima. These varying, yet similar, timescales between Bermuda and Abaco suggest that LSW may split from the traditionally perceived DWBC pathway along the western continental shelf of the Atlantic and escape into the central Atlantic through recirculation pathways, allowing this signal to reach both locations on similar timescales. The presence of dual minima at Abaco and Bermuda could also further support that LSW advects in patches rather than as a continuous mass, perhaps also a product of alternative advective-recirculation pathways where one patch was subject to one pathway while the other patch simultaneously advected along another. The outcomes of this layer-averaging approach leave room for uncertainty and do not alone provide sufficient means to gauge advective timescales, as layer-averaging tends to smooth and cover up important convective signals. To improve on the advective estimates of this layer-average approach, contrary to previous studies, we look closely within the layer and follow the advection of two LSW classes,  $\text{LSW}_{1987\text{--}1994}$  and  $\text{LSW}_{2000\text{--}2003}$ .

Figure 7 showcases the potential temperature and salinity anomalies of all four locations through time in neutral density space, with the defined Intermediate, Deep, and Abyssal layers indicated by the horizontal dashed lines. In the Labrador Sea,  $\text{LSW}_{1987\text{--}1994}$  is showcased by the extreme minima in potential temperature and salinity spanning the surface ( $\gamma_n \sim 27.87$ , isopycnal outcropped to atmosphere) to the bottom boundary of the intermediate layer,  $\gamma_n = 28.01$ . The deep  $\text{LSW}_{1987\text{--}1994}$  signal is observed to remain within this layer for approximately a decade, and warm and saline post-convective surrounding water fills the void of this class in the lower half of the intermediate layer once its signal is advected out of the Labrador Sea.  $\text{LSW}_{2000\text{--}2003}$  is observed in the Labrador Sea through a second minima in the anomalies, although only occupying the upper half of the intermediate layer and persisting for approximately 5 yr before seeing the return of post-convective, warm, and saline surrounding water. An anomalously cold and fresh feature is evident below the intermediate layer ( $\gamma_n > 28.01$ ) in the Labrador Sea stretching all the way to the seafloor ( $\gamma_n \sim 28.2$ ) spanning years 1990–2015. This is likely a response of the observed freshening of the Subpolar North Atlantic between 1960 and the late 1990s (Dickson et al., 2002), evident through the deeper layers that constrain the ISOW and DSOW water masses that are advected into the Labrador Sea from the eastern Subpolar North Atlantic. It is also possible that this deeper freshening is product of  $\text{LSW}_{1987\text{--}1994}$  spreading into the Subpolar North Atlantic, transforming into and/or mixing with ISOW and

DSOW in the eastern Subpolar North Atlantic, then recirculating back into the Labrador Basin to be observed and re-exported as such (Yashayaev, Bersch, et al., 2007; Yashayaev, van Aken, et al., 2007). The most recent convective class (>2012) is observed in the Labrador Sea data set in the upper half of the intermediate layer, however, it is not yet observed at any of the downstream hydrographic transects and is therefore not examined in this study.

The distinct convective anomaly imprints observed in the Labrador Sea ( $LSW_{1987-1994}$ ,  $LSW_{2000-2003}$ , post-convective relaxation, deeper freshening) are observed at all three downstream locations, and we can use the visual onset of these signals as advective tracers. At Line W, we observe the onset of the  $LSW_{1987-1994}$  convective signal in the mid-1990s (Figure 7). It is likely this signal would continue through the data gap spanning 1998–2001. This signal is followed by the deeper freshening signal in the deep and abyssal layers,  $LSW_{2000-2003}$  signal in the upper half of the intermediate layer (2005), and the beginnings of the major warm/saline post-convective period (2008). At Bermuda, given a longer time series, we can identify these four prominent events, most recently with the onset of the warm/saline post-convective period into present day. At Abaco, we identify the  $LSW_{1987-1994}$  signal visible after the data gap in 2001, the onset of the deep freshening in 2008, the  $LSW_{2000-2003}$  signal in the upper half of the intermediate layer (~2010), and the transition to the post-convective relaxation phase with the onset of warm and saline conditions in 2018.

### 3.2.2. Isopycnal Core Analysis

To further understand the evolution and advection of LSW along the DWBC, we identify two convective periods of interest from the source region within the defined intermediate layer: the denser LSW class formed between the years 1987–1994 in the Labrador Sea ( $LSW_{1987-1994}$ ) with its core defined along the  $\gamma_n = 27.99$  isopycnal, and the lighter LSW class formed between the years 2000–2003 in the Labrador Sea ( $LSW_{2000-2003}$ ) with its core defined along the  $\gamma_n = 27.90$  isopycnal (Figure 7). By identifying the unique convective signals of both LSW classes in the source region of the Labrador Sea (described in Section 3.1), we follow the individual advection of each LSW class as it spreads out of the Labrador Sea and into the Atlantic via the DWBC along distinct isopycnal cores. We assume constant isopycnal spreading and negligible diapycnal diffusion along the advective process. However, a  $-0.015 \text{ kg/m}^3$  neutral density shift in the data sets downstream of the source region was observed by an offset in the minima of the potential temperature and salinity signal along both isopycnals cores of 27.90 and 27.99  $\text{kg/m}^3$ . This further suggests that there may be a diapycnal mixing influence or modification of the water masses as previously discussed causing the LSW cores (i.e., minima in potential temperature and salinity) to be observed downstream of the source region along a neutral density isopycnal that is  $0.015 \text{ kg/m}^3$  lighter. To limit the impact of mixing on this advective study, and because we deemed the influence of MOW and other intermediate waters negligible to the isolation of the source region convective signal, a  $+0.015 \text{ kg/m}^3$  neutral density adjustment is applied to the Line W, Bermuda, and Abaco data sets as described in Section 2.3 to keep the isopycnal cores constant across all locations (refer to Section S1 in Supporting Information S1). The data presented throughout this study has already been subject to this density offset.

Potential temperature and salinity time series along both respective LSW cores (Figure 8) showcase the onset of each convective signal, shown as a minimum in temperature and salinity (Table 1). Looking at the deeper, denser, and more prominent  $LSW_{1987-1994}$  class, we observe advective timescales of 3 yr to Line W from the source region, 9 yr to Bermuda, and also 9 yr to Abaco based on the minima in properties. The similar scale in advective time to Bermuda and Abaco again suggest that another advective pathway is likely, perhaps one that would split from the DWBC and advect this signal to be observed in the central Atlantic and the subtropics at the same time. The lighter, shallower, and more short-lived  $LSW_{2000-2003}$  class is observed to advect on longer timescales, taking 7 yr to reach Line W, 12–14 to Bermuda, and 8–13 to Abaco.  $LSW_{2000-2003}$  minima at Abaco are observed with a rapid drop in both the temperature and salinity in 2008, followed by a more modest minimum in 2011 and 2013, although still trailing ahead of the signal observed at Bermuda by about a year. The minima in 2008 at Abaco could possibly be evidence of the first signs of  $LSW_{2000-2003}$  reaching this location from a DWBC throughflow pathway only 1 yr after reaching Line W, while other parts of this water mass could have been advected toward the Atlantic interior at the same time, delaying the second minima arrival at Abaco. Because Bermuda is observed to have longer timescales with the lighter class, it is again likely to postulate that an interior advective pathway is present, or more likely a bifurcation in DWBC advective flow somewhere between Line W and Abaco, causing these LSW signals to be observed downstream at Abaco just prior to or on similar timescales of when they are observed at Bermuda. Outside of the DWBC and hypothesized alternative-advective pathway discussed here, it is not unreasonable to question whether the LSW signals observed at Bermuda arrived from a different

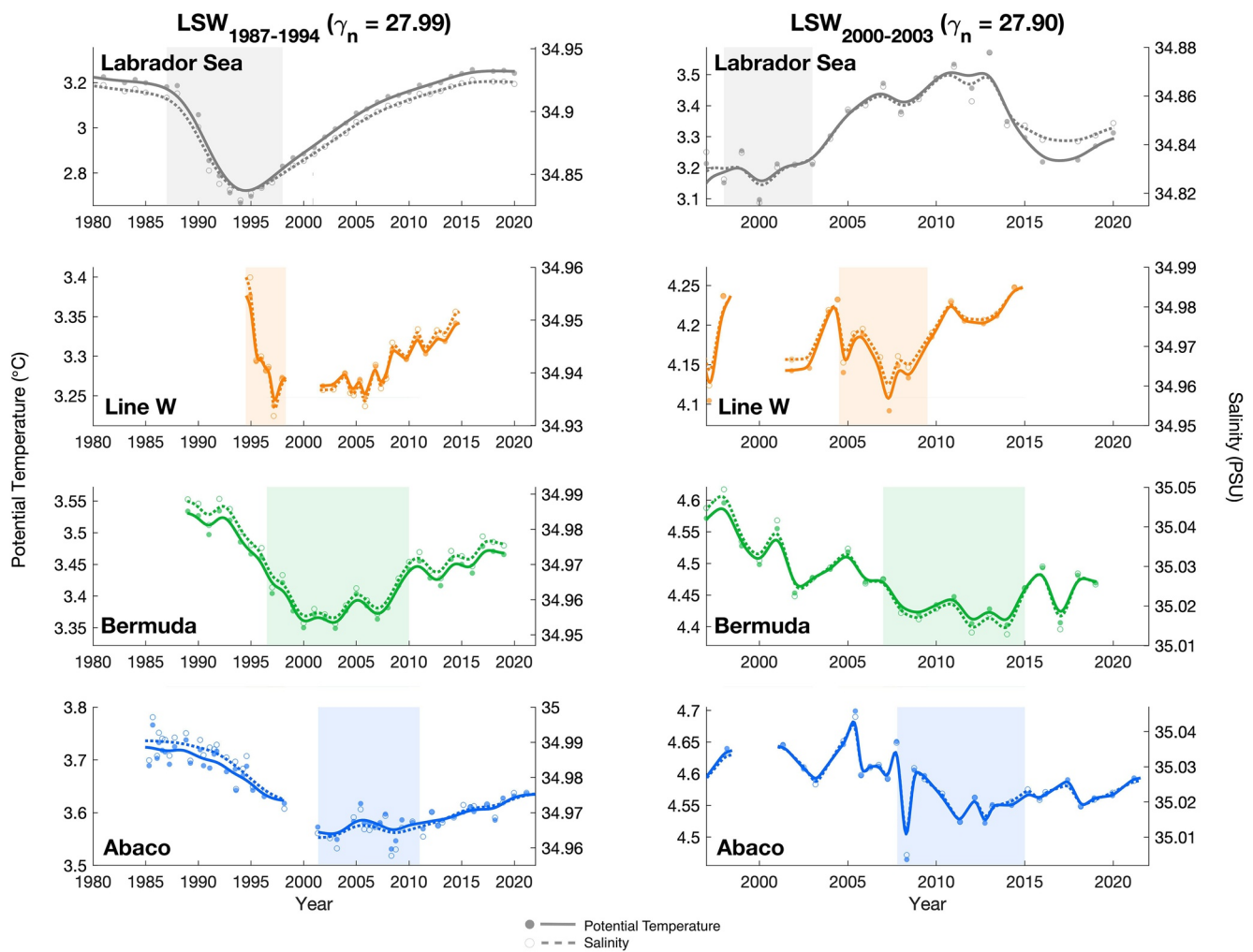


**Figure 8.** Potential temperature (solid line) and salinity (dashed line) of the isopycnal cores of LSW<sub>1987-1994</sub> (left panels) and LSW<sub>2000-2003</sub> (right panels) among all four hydrographic locations. Curves are shown smoothed and monthly interpolated, while filled (potential temperature) and open (salinity) circles mark individual unsmoothed and uninterpolated data points for reference. The shaded region represents the approximate evolution of the convective minima defined through visual assessment.

direct-interior pathway (avoiding DWBC altogether), however further research is needed to address this question. The duration of convective signals along both isopycnal levels are different when comparing observations at Line W to observations further downstream at Bermuda and Abaco. Both signals arrive at Line W with faster amplitudes and shorter durations compared to the arrival and signal duration at Bermuda and Abaco (Figure 8), and we attribute this to two factors: proximity and mixing. Line W is closest in proximity to the Labrador Sea, and the location transects a direct, one-way transport of the signal via the DWBC. Bermuda and Abaco, on the other hand, are much further away from the source region and LSW masses are likely more influenced by localized recirculation patterns along the advected route, where the likelihood of convergence, mixing, and/or entrainment with recirculated waters of the same density level makes the evolution of the signal longer and less drastic in nature.

### 3.2.3. Cross-Correlated Lag Estimates

As a third approach to determine advective timescales of LSW via the DWBC, monthly interpolated time series of salinity along both isopycnal cores of all data sets are cross-correlated to the source region providing time lag estimates in years on the onset of each LSW class convective minima signal. Original data gaps in the time series are maintained in the monthly interpolation. An autocorrelation is performed for the Labrador Sea time series (Figure 9a), where we find a decorrelation time scale of 8–10 yr, indicative that these convective

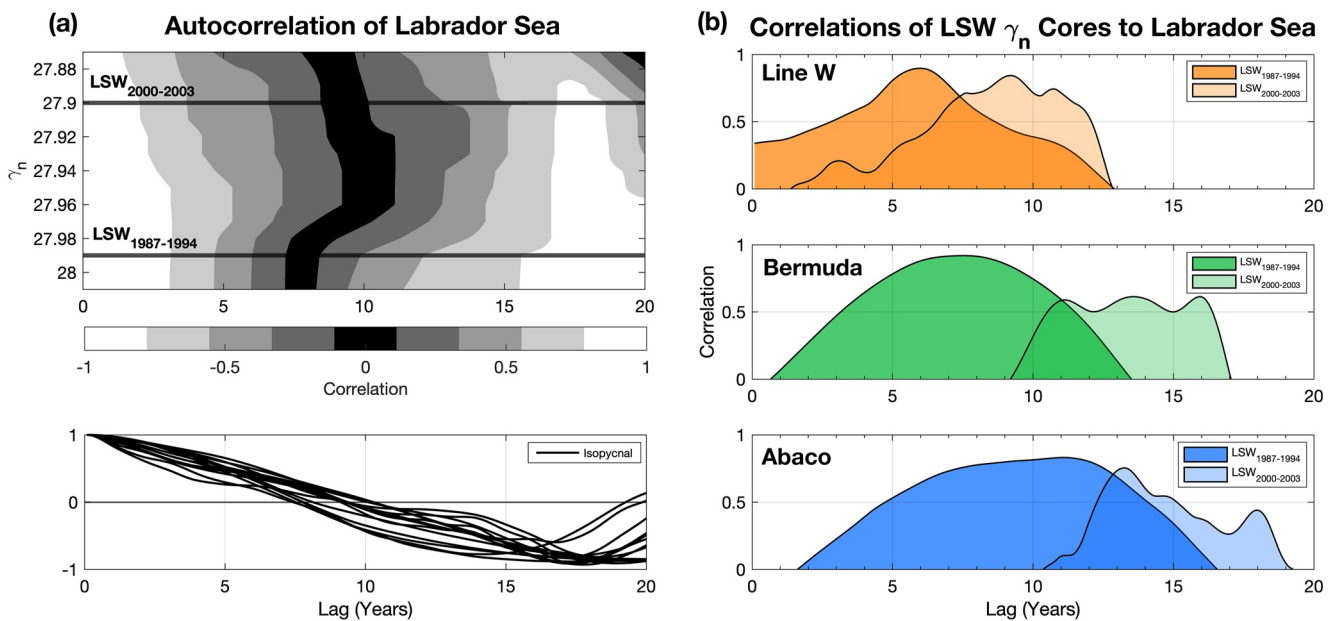


**Figure 9.** (a) Autocorrelation of the Labrador Sea time series (1970–2020), showcasing a decadal cycle to the observed convective events. Top panel shows the intermediate layer in neutral density space ( $\gamma_n = 27.87\text{--}28.01$ ), with the 0-autocorrelation corresponding to a lag of 8–10 yr, supported by the bottom panel of each isopycnal level of the layer. (b) Cross-correlations of LSW<sub>1987–1994</sub> and LSW<sub>2000–2003</sub> isopycnal cores of each time series to the Labrador Sea, where the maximum correlation indicates the advective lag time in years. Correlations are performed using monthly interpolated salinity data sets.

events prevail on decadal timescales. Based on the correlation of each time series to that of the Labrador Sea (Figure 9b), we find the LSW<sub>1987–1994</sub> core to advect on timescales of 6 yr at Line W, 8 yr at Bermuda, and 11 yr at Abaco. The correlations of Line W and Abaco are, however, influenced by the data gaps in both time series from 1998 to 2001. LSW<sub>2000–2003</sub> is observed to advect on longer and more ambiguous timescales, as supported by other approaches; 9 yr at Line W, 11–16 yr at Bermuda, and 13–18 yr at Abaco. Correlations using potential temperature produced similar results and are not shown. The increased time lag in the LSW<sub>2000–2003</sub> class further downstream continues to suggest that this lighter, shallower class was subject to an alternative advective pathway, which may be why Bermuda and Abaco show similar timescales despite being about 1,400 km apart.

Cross-correlations across the entire intermediate layer are shown in Figure 10 in time-density space, broken into the lower and upper intermediate layer components showcasing the LSW<sub>1987–1994</sub> and LSW<sub>2000–2003</sub> classes, respectively. Correlations are performed again using monthly interpolated salinity time series of each location to that of the Labrador Sea time series across the density range of the intermediate layer, where the maximum in correlation indicates the lag time of the signal in years. Correlations using the monthly interpolated potential temperature time series resulted in similar findings (not shown). Cross-correlations of LSW<sub>2000–2003</sub> and respective upper intermediate layer (Figure 10, right) are used with a truncated Labrador Sea source region data set beginning in 1994, where the LSW<sub>1987–1994</sub> signal is masked from the upper intermediate layer, as it would skew the correlation. Lag results continue to confirm the two interesting findings. First, like the correlations of the individual cores, looking at the full layer also showcases the denser LSW<sub>1987–1994</sub> class arriving at Bermuda just prior to or at the same time as arriving at Abaco, further suggesting that there is an alternative or recirculated DWBC pathway that brings LSW to the Atlantic interior. Second, the lighter LSW<sub>2000–2003</sub> class advects on longer timescales than that of LSW<sub>1987–1994</sub>. This suggests that shallower LSW masses are more likely to be advected towards the basin interior adding to their advective timescales. A bifurcation and two subsequent routes of the DWBC advective pathway are quite likely to exist based solely on the hydrographic data presented in this study: the classically understood direct route along the western basin which bypasses Bermuda, and a deflective pathway that shoots out into the central Atlantic prior to rejoining the western slope. Both LSW classes could have been subjected to the latter based on the arrival and duration of the convective signals, however, further investigation is needed for a definitive answer on the existence of a direct DWBC pathway and its role in LSW advection.



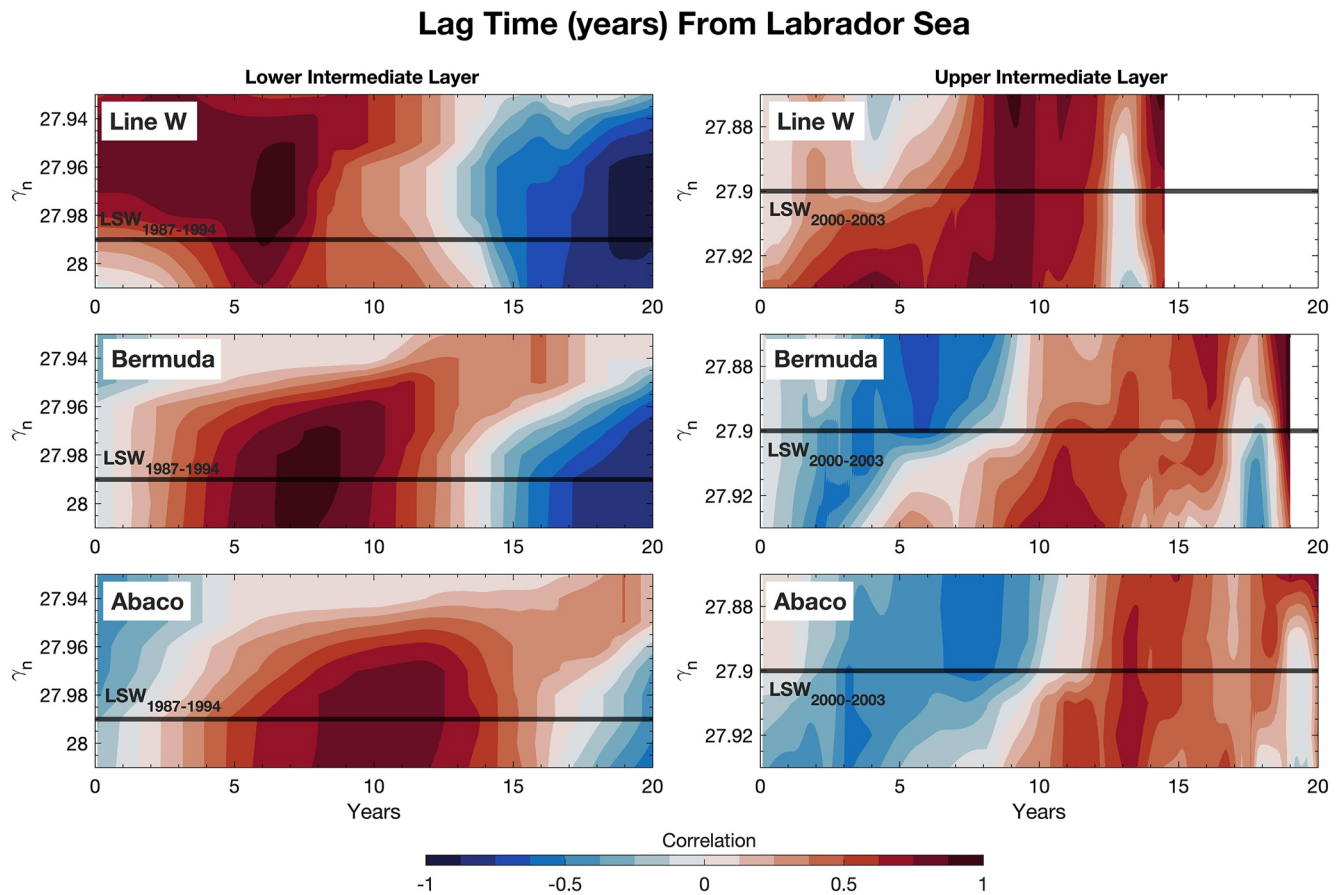


**Figure 10.** Cross-correlations of Line W (top), Bermuda (middle), and Abaco (bottom) salinity data sets to the Labrador Sea salinity source data set in neutral density space with time lag in years shown along the x-axes. Correlations are performed for the lower intermediate layer showcasing the LSW<sub>1987–1994</sub> core signal along the highlighted  $\gamma_n = 27.99$  isopycnal (left panels) and the upper intermediate layer (right panels) showcasing the LSW<sub>2000–2003</sub> core signal along the highlighted  $\gamma_n = 27.90$  isopycnal. Correlations of the latter-LSW<sub>2000–2003</sub> signal are trimmed due to limitation in the time series availability. For reference, the  $\gamma_n = 27.99$  isopycnal is found at approximately 2,000 m (Line W), 1,900 m (Bermuda), and 2,000 m (Abaco); the  $\gamma_n = 27.90$  isopycnal is found at approximately 1,000 m (Line W), 1,400 m (Bermuda), and 1,300 m (Abaco).

#### 4. Discussion and Conclusions: Updated Advective Timescales and DWBC Pathways

This study presents a comprehensive analysis of LSW advection along the DWBC in the North Atlantic Ocean as it incorporates multiple locations along the transport pathway, building upon previous studies that compared trends in hydrographic time series to the formation region of LSW, the Labrador Sea (Le Bras et al., 2017; Molinari et al., 1998; van Sebille et al., 2011). Using geographically cohesive neutral density definitions on both a broad and fine scale, we defined an intermediate NADW layer and isolated specific LSW classes therein. Through various approaches such as layer-averaging (Section 3.2.1), isopycnal core analysis (Section 3.2.2), and cross-correlation analysis (Section 3.2.3), the advection of LSW via the DWBC was observed through the passage of convective signals and advective timescales were estimated (summarized in Table 2).

Multi-year observations of LSW at several locations across the western North Atlantic indicate that recirculation or deflection pathways branching from the DWBC are likely to exist. This is evident by the observed presence of LSW in the Bermuda Basin, and the advective timescales that support this spreading trajectory. While layer averaging of the intermediate layer (Section 3.2.1) provides a broad look at the onset of the convective signal at each location, we find here that the intense LSW<sub>1987–1994</sub> convective signal dominates the layer, and the averaged minima across all data sets reflect solely that signal, muting any others (LSW<sub>2000–2003</sub>, e.g.). The onset of the minima in the averaged intermediate layer gives advective timescales of 3 yr to Line W (39°N), 9–14 yr to Bermuda (32°N), and 9–14 yr to Abaco (26.5°N). Looking at tendencies in potential temperature and salinity anomalies (Figure 7) highlights the equatorward propagation of LSW<sub>1987–1994</sub>, LSW<sub>2000–2003</sub>, post-convective

**Table 2**

*Summary of Advective Timescales in Years From the Source Region in the Labrador Sea to Each Hydrographic Location Inferred Through the Three Approaches Presented in This Study: [1] Minima of the Averaged Intermediate Layer, [2] Minima of the LSW<sub>1987–1994</sub> and LSW<sub>2000–2003</sub> Isopycnal Cores, and [3] Cross-Correlations of the Each Labrador Sea Water (LSW) Core As Well as the Lower and Upper Intermediate Layer Pertaining to the LSW Cores*

| Advective timescale from Labrador Sea (years)  |                         |                          |                          |
|--|-------------------------|--------------------------|--------------------------|
| Advective timescale approach:                  | Line W                  | Bermuda                  | Abaco                    |
| [1] Intermediate layer average                 | 3                       | 9–14                     | 9–14                     |
| [2] LSW <sub>1987–1994</sub> core minima       | 3                       | 9                        | 9                        |
| LSW <sub>2000–2003</sub> core minima           | 7                       | 12–14                    | 8, 11–13                 |
| [3] Cross-correlation LSW <sub>1987–1994</sub> | 6 <sub>(core)</sub>     | 8 <sub>(core)</sub>      | 11 <sub>(core)</sub>     |
|  | 6 <sub>(layer)</sub>    | 8 <sub>(layer)</sub>     | 10 <sub>(layer)</sub>    |
| Cross-correlation LSW <sub>2000–2003</sub>     | 9 <sub>(core)</sub>     | 11–16 <sub>(core)</sub>  | 13–18 <sub>(core)</sub>  |
|  | 5–11 <sub>(layer)</sub> | 10–15 <sub>(layer)</sub> | 11–18 <sub>(layer)</sub> |
| Previous estimates                             | 3–7 <sup>a</sup>        | 6 <sup>b,c</sup>         | 10 <sup>d,e</sup>        |

Note. LSW<sub>2000–2003</sub> is observed to advect on longer and varying timescales compared to LSW<sub>1987–1994</sub>. Advective estimates of LSW from previous studies are shown for comparison.

<sup>a</sup>Le Bras et al. (2017). <sup>b</sup>Curry and McCartney (1996). <sup>c</sup>Curry et al. (1998). <sup>d</sup>Molinari et al. (1998). <sup>e</sup>van Sebille et al. (2011).

relaxation, and the deep-freshening signals at all four hydrographic locations. Most importantly, these features are observed at Bermuda in the central Atlantic just prior to or at similar timescales to being observed downstream at Abaco, suggesting that LSW and associated signals may arrive from the central Atlantic via an interior pathway.

By isolating two of the LSW classes, LSW<sub>1987–1994</sub> and LSW<sub>2000–2003</sub>, improved advective timescales can be ascertained. Through the second and third approaches of estimating advective timescales (Section 3.2.2, cross-correlations in Section 3.2.3), we find that the deeper LSW<sub>1987–1994</sub> class advected in an unconventional route, inferred from the onset of convective minima (Figure 8) and advective lag times in Figures 9b and 10 by the passage of the signal through Line W, then Bermuda, and lastly through Abaco. This finding continues to support the hypothesis of an alternative advective pathway, where LSW is deflected toward the Atlantic interior prior to returning to the continental slope to be observed at 26.5°N. LSW<sub>2000–2003</sub> was also shown to follow an alternative advective route, on longer timescales however, perhaps indeed validating this bifurcation and alternative-advective pathway hypothesis where this water mass spent longer in the Atlantic interior. Advective timescales for both LSW classes from the Labrador Sea to Line W suggest approximately 7 yr, however, this is a bit uncertain given the gap in data during the LSW<sub>1987–1994</sub> signal propagation.

We find the arrival of both convective signals to be of greater amplitude and advect with shorter duration at Line W compared to the downstream locations of Bermuda and Abaco. We attribute this to the close proximity of Line W to the Labrador Sea and the direct, one-way, un-recirculated transit the DWBC facilitates on that hydrographic location. Bermuda and Abaco, on the

other hand, are much further away from the source region and LSW convective signals are likely influenced by interior recirculations, where the possibility of convergence, mixing, and/or entrainment with recirculated waters of the same density makes the evolution of the signal longer and less pronounced, yet still observable. We do not dismiss the influence of other fresher sources impacting the freshening of the LSW signal, however, it is more likely sources of higher salinity along the same density level along the advective pathway, such as MOW, which affect the overall salinity of the LSW signal. The influence of other subpolar waters, the Gulf Stream, and MOW are more likely to increase the salinity of the LSW convective signal rather than lower it. At Abaco and Bermuda, for example, we observe a modulation of three types of waters: a true fresh LSW mass, true salty MOW, and an intermediate mix between the two; the influence of MOW and other water masses of higher salinity are reduced via the data cleaning scheme implemented for this study to focus solely on LSW advection. The constant shift in neutral density that is observed (−0.015 kg/m<sup>3</sup>) at all locations downstream of the Labrador Sea also supports the plausibility of entrainment. The fact that the offset remains nearly constant outside of the Labrador Sea suggests that mixing of warmer and more saline intermediate Atlantic waters with LSW, and therefore the most notable transformation, occurs in the upstream part of the DWBC advective pathway prior to reaching Line W. Comparison of vertical temperature and salinity profiles for these regions supports this assumption solely based on the shift in the LSW core density. As previously described, a constant neutral density offset was applied to Line W, Bermuda, and Abaco data sets to minimize the impacts of mixing.

Variability in advective timescale is observed after LSW passes through Line W, as seen in Bermuda and Abaco locations, implying that the alternative pathway junction exists south of 39°N. It is likely the DWBC bifurcation location exists at the Gulf Stream-DWBC crossover region off the coast of Cape Hatteras (36°N), as has been supported through many recent and past works through theory, Lagrangian, and stream function approaches (Andres et al., 2018; Biló & Johns, 2019; Bower & Hunt, 2000a, 2000b; Bower et al., 2011; Spall, 1996a, 1996b). To look at spreading pathways in the North Atlantic, we employ use of adjusted geostrophic velocities derived from Argo and altimetry measurements (Schmid, 2014) averaged over the years 2000–2010 at 1,000, 1,500 m (approximate LSW<sub>2000–2003</sub> core depth), 1,750 m (approximate mid-intermediate layer depth), and 2,000 m (approximate LSW<sub>1987–1994</sub> core depth; Figure 11). We speculate that the dynamics of the Gulf Stream-DWBC

2000-2010 Mean Flow

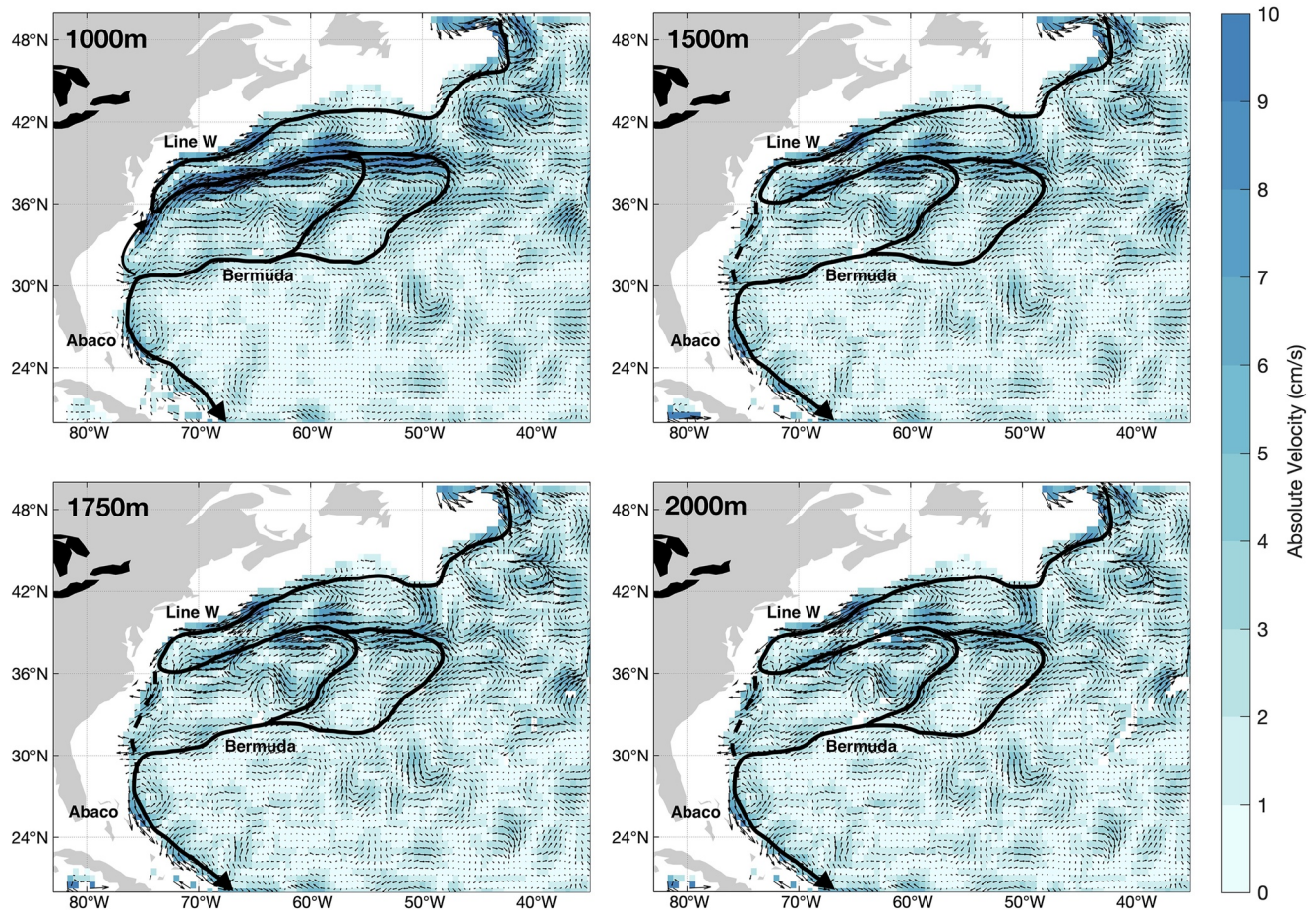


**Figure 11.** Adjusted geostrophic velocities derived from Argo and altimetry using the climatological velocity field from Argo trajectories as the reference velocity (Schmid, 2014). Argo dynamic height profiles and SSH from altimetry are used to derive synthetic dynamic height profiles on a  $0.5^\circ$  grid. These profiles are then used to derive the horizontal geostrophic velocity, followed by the barotropic adjustment. The resulting velocity was averaged over the years 2000–2010 at 1,000, 1,500 (approximate  $LSW_{2000-2003}$  depth), 1,750 m (mid-intermediate layer depth), and 2,000 m (approximate  $LSW_{1987-1994}$  depth) levels. Vectors indicate flow direction, while color gradient represents the absolute velocity in cm/s. Black lines showcase Deep Western Boundary Current (DWBC) flow pathways dictated by vector direction, showcasing an interior pathway that bifurcates from the continental shelf at approximately  $36^\circ N$  observed at all depth levels. The dashed throughflow pathway along the continental shelf south of  $36^\circ N$  remains uncertain and unresolved from the given Argo trajectories.

crossover region play a large role in the circulation patterns observed. At all depth levels we observe a deflection in the DWBC near Cape Hatteras, generating a recirculation gyre that extends out to  $50^\circ W$  then rejoins the continental slope at  $30^\circ N$ , passing Bermuda in the process. This deflection is likely influenced by upper-ocean dynamics of the Gulf Stream extension. It is difficult to ascertain whether a bifurcation in the DWBC exists near Cape Hatteras rather than a complete deflection toward the interior. If a bifurcation indeed exists, then a southward DWBC throughflow between  $36^\circ$  and  $30^\circ N$  may still be a viable advective pathway. As shown in Figure 11, at 1,000 m, a northward flow is observed in this region along the continental shelf, likely influenced by the northward flow of the upper-ocean Gulf Stream dynamics. Below 1,000 m, Argo coverage along the continental shelf is rather sparse, but vectors indicate that there may be some leakage in the DWBC that bypasses the deflection and continues equatorward along the continental slope opposite of the poleward-flowing Gulf Stream. These findings, in addition to the advective timescales estimated from the hydrographic data, provide observational evidence supporting the hypothesis of a bifurcated DWBC and alternative interior advective pathway.

The updated broad-scale, cohesive, and all-encompassing NADW density definitions presented here serve to benefit the greater AMOC community when it comes to understanding advection of LSW, as the defined density range of this water mass can alter findings by including signals that were previously neglected. Modeling

efforts to understand Labrador Sea convection, Subpolar North Atlantic circulation, atmospheric forcing, and overturning circulation among others have used a multitude of methods and parameterizations to characterize LSW (Chanut et al., 2008; Li et al., 2019; Luo et al., 2011; Menary et al., 2020; Pickart & Spall, 2007; Schott et al., 2009; Zhang & Thomas, 2021). AMOC modeling efforts must consider the complexity of LSW formation and resulting characterization, as subtle changes to input parameters may challenge the fidelity of models or generate inviable outcomes when it comes to assessing the true role of LSW on the mechanisms and pathways of the lower-limb of AMOC.

The advective timescales presented herein are shown to be longer and more variable than those of previous studies, but are estimated using updated observational data sets and more robust approaches. These longer advective timescales could be a result of the broad hydrographic analysis, covering a larger geographic range than previous studies and incorporating numerous hydrographic locations serving to render a broader analysis. The longer advective scales could also be a result of the recent advancement in observing systems, longer time series, and enhanced data sets. Past advective timescales could therefore have been misrepresented due to improper water mass classification or sparse hydrographic data, such as in the case of Abaco in previous studies. Findings of this study highlight the cohesiveness of LSW advection out of the Subpolar North Atlantic, as the magnitude of each convective signal is flagrant enough to be used as an advective tracer. Continued investigation of alternative advective pathways into the Atlantic basin interior through sustained hydrographic monitoring programs are needed to further understand the role of these pathways on the lower-limb of AMOC, however, the findings of this study firmly suggest that these interior pathways may play a large role in the advection of subpolar water masses to the tropics in the North Atlantic.

### Data Availability Statement

The Labrador Sea hydrographic ship survey based data set, maintained and provided by I. Yashayaev (available from the CLIVAR and Carbon Hydrographic Data Office (CCHDO; <https://cchdo.ucsd.edu/search?q=AR07W>)), profiling Argo float (available from the Argo Global Data Assembly Center (GDAC; [<ftp://usgodae.org/pub/outgoing/argo/>] and <ftp://ftp.ifremer.fr/ifremer/argo/>]), and other historical and recent Labrador Sea observations from various sources (available from the NOAA National Centers for Environmental Information World Ocean Database; <https://www.ncei.noaa.gov/products/world-ocean-database>) were assembled, thoroughly quality controlled, calibrated and analyzed as part of the Deep-Ocean Observations and Research Synthesis (DOORS) program, a Canadian successor of the World Ocean Circulation Experiment (WOCE), initiated and led by the Bedford Institute of Oceanography of Fisheries and Oceans Canada. Line W hydrographic data is made freely available from Woods Hole Oceanographic Institute [<https://scienceweb.whoi.edu/linew/index.php>]. The Bermuda basin hydrographic data set was freely sourced from the Bermuda Atlantic Time Series and Hydrostation S programs through the Bermuda Institute of Oceanography [<http://bats.bios.edu/data/>]. Abaco hydrographic data of the 26.5°N NOAA Western Boundary Time series Program is supplied by the NOAA Atlantic Oceanographic and Meteorological Laboratory (AOML) and is publicly available through the NOAA National Centers for Environmental Information World Ocean Database [<https://www.ncei.noaa.gov/products/world-ocean-database>, <https://www.aoml.noaa.gov/phod/wbts/data.php>]. Adjusted geostrophic velocities were derived by C. Schmid using Argo float data from the Global Data Assembly Centre [<http://doi.org/10.17882/42182>] and altimetry data as described in Schmid (2014); data is available upon request. The Ssalto/Duacs altimeter products were produced and distributed by the Copernicus Marine and Environmental Monitoring Service (CMEMS) [<https://www.marine.copernicus.eu>]. As part of the Global Ocean Observing System, Argo data are collected and made freely available by the International Argo Program and the national programs that contribute to it [<https://argo.ucsd.edu>, <https://argo.jcommops.org>, <https://www.ocean-ops.org>].

### References

- Andres, M., Muglia, M., Bahr, F., & Bane, J. (2018). Continuous flow of upper Labrador Sea Water around Cape Hatteras. *Scientific Reports*, 8(1), 4494. <https://doi.org/10.1038/s41598-018-22758-z>
- BATS Methods. (1997). Bermuda Institute of Oceanography. Online Report. Retrieved from [http://bats.bios.edu/wp-content/uploads/2017/07/report\\_methods.pdf](http://bats.bios.edu/wp-content/uploads/2017/07/report_methods.pdf)
- Biló, T. C., & Johns, W. E. (2019). Interior pathways of Labrador Sea Water in the North Atlantic from the Argo perspective. *Geophysical Research Letters*, 46(6), 3340–3348. <https://doi.org/10.1029/2018GL081439>
- Biló, T. C., & Johns, W. E. (2020). The Deep Western Boundary Current and adjacent interior circulation at 24°–30°N: Mean structure and mesoscale variability. *Journal of Physical Oceanography*, 50(9), 2735–2758. <https://doi.org/10.1175/JPO-D-20-0094.1>

### Acknowledgments

The authors thank the reviewers for their insightful comments and suggestions. A sincere thanks is extended to the individuals of each institution involved in the sea-going collection, calibration, and processing of the hydrographic data presented here in this study. This research was supported by the University of Miami Rosenstiel School of Marine, Atmospheric, and Earth Science and by the NOAA Atlantic Oceanographic and Meteorological Laboratory (AOML), and it was carried out in part under the auspices of the Cooperative Institute for Marine and Atmospheric Studies, a Cooperative Institute of the University of Miami and NOAA, cooperative agreement #NA20OAR4320472. The 26.5°N NOAA Western Boundary Time series project (WBTS) is supported by the US NOAA Climate Program Office—Global Ocean Monitoring and Observing Program (FundRef #100007298) and by NOAA AOML. DLV and JH were also supported by the WBTS project and by NOAA AOML; DLV was also supported by NOAA Climate Variability and Predictability program (Grant NA20OAR4310407).

- Blaker, A. T., Hirschi, J. J. M., McCarthy, G., Sinha, B., Taws, S., Marsh, R., et al. (2015). Historical analogs of the recent extreme minima observed in the Atlantic Meridional Overturning Circulation at 26°N. *Climate Dynamics*, *44*(1–2), 457–473. <https://doi.org/10.1007/s00382-014-2274-6>
- Bower, A. S., & Hunt, H. D. (2000a). Lagrangian observations of the Deep Western Boundary Current in the North Atlantic Ocean, Part I: Large-scale pathways and spreading rates. *Journal of Physical Oceanography*, *30*(5), 764–783. [https://doi.org/10.1175/1520-0485\(2000\)030<0764:LOOTDW>2.0.CO;2](https://doi.org/10.1175/1520-0485(2000)030<0764:LOOTDW>2.0.CO;2)
- Bower, A. S., & Hunt, H. D. (2000b). Lagrangian observations of the Deep Western Boundary Current in the North Atlantic Ocean, Part II: The Gulf Stream-Deep Western Boundary Current crossover. *Journal of Physical Oceanography*, *30*(5), 784–804. [https://doi.org/10.1175/1520-0485\(2000\)030<0784:lOOTDW>2.0.CO;2](https://doi.org/10.1175/1520-0485(2000)030<0784:lOOTDW>2.0.CO;2)
- Bower, A., Lozier, S., Biastoch, A., Drouin, K., Foukal, N., Furey, H., et al. (2019). Lagrangian views of the pathways of the Atlantic Meridional Overturning Circulation. *Journal of Geophysical Research: Oceans*, *124*(8), 5313–5335. <https://doi.org/10.1029/2019JC015014>
- Bower, A., Lozier, S., & Gary, S. (2011). Export of Labrador Sea Water from the Subpolar North Atlantic: A Lagrangian perspective. *Deep Sea Research Part II: Topical Studies in Oceanography*, *58*(17–18), 1798–1818. <https://doi.org/10.1016/j.dsr2.2010.10.060>
- Bower, A. S., Lozier, S. M., Gary, S. F., & Böning, C. W. (2009). Interior pathways of the North Atlantic Meridional Overturning Circulation. *Nature*, *459*(7244), 243. <https://doi.org/10.1038/nature07979>
- Bryden, H. L., Johns, W. E., & Saunders, P. M. (2005). Deep Western Boundary Current east of Abaco: Mean structure and transport. *Journal of Marine Research*, *63*(1), 35–57. <https://doi.org/10.1357/0022240053693806>
- Chanut, J., Barnier, B., Large, W., Debreu, L., Penduff, T., Molines, J. M., & Mathiot, P. (2008). Mesoscale eddies in the Labrador Sea and their contribution to convection and restratification. *Journal of Physical Oceanography*, *38*(8), 1617–1643. <https://doi.org/10.1175/2008JPO3485.1>
- Cunningham, S. A., & Haine, T. W. N. (1995). Labrador Sea Water in the Eastern North Atlantic. Part I: A synoptic circulation inferred from a minimum in potential vorticity. *Journal of Physical Oceanography*, *25*(4), 649–665. [https://doi.org/10.1175/1520-0485\(1995\)025<0649:lsuite>2.0.co;2](https://doi.org/10.1175/1520-0485(1995)025<0649:lsuite>2.0.co;2)
- Cunningham, S. A., Kanzow, T., Rayner, D., Baringer, M. O., Johns, W. E., Marotzke, J., et al. (2007). Temporal variability of the Atlantic Meridional Overturning Circulation at 26.5°N. *Science*, *317*(5840), 935–938. <https://doi.org/10.1126/science.1141304>
- Curry, R. G., & McCartney, M. S. (1996). Labrador Sea Water carries northern climate signal south. *Oceanus-Woods Hole Mass*, *39*(4), 24–28. [https://www.whoi.edu/cms/files/dfino/2005/4/v39n2-curry\\_2167.pdf](https://www.whoi.edu/cms/files/dfino/2005/4/v39n2-curry_2167.pdf)
- Curry, R. G., McCartney, M., & Joyce, T. (1998). Oceanic transport of subpolar climate signals to mid-depth subtropical waters. *Nature*, *391*(6667), 575–577. <https://doi.org/10.1038/35356>
- Dickson, B., Yashayaev, I., Meincke, J., Turrell, B., Dye, S., & Holtfort, J. (2002). Rapid freshening of the deep North Atlantic Ocean over the past four decades. *Nature*, *416*(6883), 832–837. <https://doi.org/10.1038/416832a>
- Dukhovskoy, D. S., Yashayaev, I., Proshutinsky, A., Bamber, J. L., Bashmachnikov, I. L., Chassignet, E. P., et al. (2019). Role of Greenland freshwater anomaly in the recent freshening of the subpolar North Atlantic. *Journal of Geophysical Research: Oceans*, *124*(5), 3333–3360. <https://doi.org/10.1029/2018JC014686>
- Fine, R. A., & Molinari, R. L. (1988). A continuous Deep Western Boundary Current between Abaco (26.5°N) and Barbados (13°N). *Deep-Sea Research-Part A*, *35*(9), 1441–1450. [https://doi.org/10.1016/0198-0149\(88\)90096-9](https://doi.org/10.1016/0198-0149(88)90096-9)
- Fine, R. A., Rhein, M., & Andrié, C. (2002). Using a CFC effective age to estimate propagation and storage of climate anomalies in the deep western North Atlantic Ocean. *Geophysical Research Letters*, *29*(24), 2227. <https://doi.org/10.1029/2002GL015618>
- Fröb, F., Olsen, A., Våge, K., Moore, G. W. K., Yashayaev, I., Jeansson, E., & Rajasakaren, B. (2016). Irminger Sea deep convection injects oxygen and anthropogenic carbon to the ocean interior. *Nature Communications*, *7*(1), 13244. <https://doi.org/10.1038/ncomms13244>
- Gary, S. F., Lozier, S. M., Biastoch, A., & Böning, C. W. (2012). Reconciling tracer and float observations of the export pathways of Labrador Sea Water. *Geophysical Research Letters*, *39*(24), L24606. <https://doi.org/10.1029/2012GL053978>
- Gary, S. F., Lozier, S. M., Böning, C. W., & Biastoch, A. (2011). Deciphering the pathways for the deep limb of the meridional overturning circulation. *Deep Sea Research Part II: Topical Studies in Oceanography*, *58*(17–18), 1781–1797. <https://doi.org/10.1016/j.dsr2.2010.10.059>
- Hall, M. M., Joyce, T. M., Pickart, R. S., Smethie, W. M., & Torres, D. J. (2004). Zonal circulation across 52°W in the North Atlantic. *Journal of Geophysical Research*, *109*(C11), C11008. <https://doi.org/10.1029/2003JC002103>
- Handmann, P., Fischer, J., Visbeck, M., Karstensen, J., Biastoch, A., Böning, C., & Patara, L. (2018). The Deep Western Boundary Current in the Labrador Sea from observations and a high-resolution model. *Journal of Geophysical Research: Oceans*, *123*(4), 2829–2850. <https://doi.org/10.1002/2017jc013702>
- Holliday, N. P., Bersch, M., Berx, B., Chafik, L., Cunningham, S., Florindo-Lopez, C., et al. (2020). Ocean circulation causes the largest freshening event for 120 yr in eastern subpolar North Atlantic. *Nature Communications*, *11*(585), 585. <https://doi.org/10.1038/s41467-020-14474-y>
- Hooper, J. A., Baringer, M. O., & Smith, R. H. (2020). Hydrographic measurements collected aboard the NOAA Ship Ronald H. Brown, 23 February to 1 March 2018: Western Boundary Time Series cruise RB1801 (WB1802). NOAA Data Report, OAR-AOML-79 (p. 118). <https://doi.org/10.25923/mb6v-jg14>
- Jackett, D. R., & McDougall, T. J. (1997). A neutral density variable for the World's Oceans. *Journal of Physical Oceanography*, *27*(2), 237–263. [https://doi.org/10.1175/1520-0485\(1997\)027<0237:ANDVFT>2.0.CO;2](https://doi.org/10.1175/1520-0485(1997)027<0237:ANDVFT>2.0.CO;2)
- Johns, W. E., Baringer, M. O., Beal, L. M., Cunningham, S. A., Kanzow, T., Bryden, H. L., et al. (2011). Continuous, array-based estimates of Atlantic Ocean heat transport at 26.5°N. *Journal of Climate*, *24*(10), 2429–2449. <https://doi.org/10.1175/2010JCLI3997.1>
- Johns, W. E., Beal, L. M., Baringer, M. O., Molina, J. R., Cunningham, S. A., Kanzow, T., & Rayner, D. (2008). Variability of shallow and Deep Western Boundary Currents off the Bahamas during 2004–2005: Results from the 26°N RAPID-MOC Array. *Journal of Physical Oceanography*, *38*(3), 605–623. <https://doi.org/10.1175/2007JPO3791.1>
- Kanzow, T., Cunningham, S. A., Rayner, D., Hirschi, J. J. M., Johns, W. E., Baringer, M. O., et al. (2007). Observed flow compensation associated with the MOC at 26.5°N in the Atlantic. *Science*, *317*(5840), 938–941. <https://doi.org/10.1126/science.1141293>
- Kieke, D., Jochumsen, K., Schneider, L., Yashayaev, I., Greenan, B. J., Serra, N., et al. (2016). *The spreading of Labrador Sea Water from the Labrador Sea to the Newfoundland Basin*. American Geophysical Union, Ocean Sciences Meeting 2016 (p. PO53A-03).
- Kieke, D., Rhein, M., Stramma, L., Smethie, W. M., LeBel, D. A., & Zenk, W. (2006). Changes in CFC inventories and formation rates of upper Labrador Sea Water, 1997–2001. *Journal of Physical Oceanography*, *36*(1), 64–86. <https://doi.org/10.1175/jpo2814.1>
- Kieke, D., & Yashayaev, I. (2015). Studies of Labrador Sea Water formation and variability in the subpolar North Atlantic in the light of international partnership and collaboration. *Progress in Oceanography*, *132*, 220–232. <https://doi.org/10.1016/j.pocan.2014.12.010>
- Lazier, J., Hendry, R., Clarke, A., Yashayaev, I., & Rhines, P. (2002). Convection and restratification in the Labrador Sea, 1990–2000. *Deep Sea Research Part I: Oceanographic Research Papers*, *49*(10), 1819–1835. [https://doi.org/10.1016/S0967-0637\(02\)00064-X](https://doi.org/10.1016/S0967-0637(02)00064-X)
- Lazier, J. R. N. (1980). Oceanographic conditions at Ocean Weather Ship Bravo, 1964–1974. *Atmosphere-Ocean*, *18*(3), 227–238. <https://doi.org/10.1080/07055900.1980.9649089>

- Le Bras, I. A., Yashayaev, I., & Toole, J. M. (2017). Tracking Labrador Sea Water property signals along the Deep Western Boundary Current. *Journal of Geophysical Research: Oceans*, 122(7), 5348–5366. <https://doi.org/10.1002/2017JC012921>
- Li, F., Lozier, M. S., Danabasoglu, G., Holliday, N. P., Kwon, Y., Romanou, A., et al. (2019). Local and downstream relationships between Labrador Sea Water volume and North Atlantic Meridional Overturning Circulation variability. *Journal of Climate*, 32(13), 3883–3898. <https://doi.org/10.1175/JCLI-D-18-0735.1>
- Lozier, M. S., Li, F., Bacon, S., Bahr, F., Bower, A. S., Cunningham, S. A., et al. (2019). A sea change in our view of overturning in the subpolar North Atlantic. *Science*, 363(6426), 516–521. <https://doi.org/10.1126/science.aau6592>
- Luo, H., Bracco, A., & Di Lorenzo, E. (2011). The interannual variability of the surface eddy kinetic energy in the Labrador Sea. *Progress in Oceanography*, 91(3), 295–311. <https://doi.org/10.1016/j.pocean.2011.01.006>
- McCartney, M. S. (1992). Recirculating components to the deep boundary current of the northern North Atlantic. *Progress in Oceanography*, 29(4), 283–383. [https://doi.org/10.1016/0079-6611\(92\)90006-L](https://doi.org/10.1016/0079-6611(92)90006-L)
- Meinen, C. S., Baringer, M. O., & Garzoli, S. L. (2006). Variability in Deep Western Boundary Current transports: Preliminary results from 26.5°N in the Atlantic. *Geophysical Research Letters*, 33(17), L17610. <https://doi.org/10.1029/2006GL026965>
- Meinen, C. S., Garzoli, S. L., Johns, W. E., & Baringer, M. O. (2004). Transport variability of the Deep Western Boundary Current and the Antilles Current off Abaco Island, Bahamas. *Deep Sea Research—Part I*, 51(11), 1397–1415. <https://doi.org/10.1016/j.dsr.2004.07.007>
- Menary, M. B., Jackson, L. C., & Lozier, M. S. (2020). Reconciling the relationship between the AMOC and Labrador Sea in OSNAP observations and climate models. *Geophysical Research Letters*, 47(18), e2020GL089793. <https://doi.org/10.1029/2020GL089793>
- Molinari, R. L., Fine, R. A., & Johns, E. (1992). The Deep Western Boundary Current in the tropical North Atlantic Ocean. *Deep Sea Research—Part A*, 39(11–12), 1967–1984. [https://doi.org/10.1016/0198-0149\(92\)90008-H](https://doi.org/10.1016/0198-0149(92)90008-H)
- Molinari, R. L., Fine, R. A., Wilson, W. D., Curry, R. G., Abell, J., & McCartney, M. S. (1998). The arrival of recently formed Labrador Sea Water in the Deep Western Boundary Current at 26.5°N. *Geophysical Research Letters*, 25(13), 2249–2252. <https://doi.org/10.1029/98GL01853>
- Peña-Molino, B., Joyce, T. M., & Toole, J. M. (2011). Recent changes in the Labrador Sea Water within the Deep Western Boundary Current southeast of Cape Cod. *Deep Sea Research Part I: Oceanographic Research Papers*, 58(10), 1019–1030. <https://doi.org/10.1016/j.dsr.2011.07.006>
- Peña-Molino, B., Joyce, T. M., & Toole, J. M. (2012). Variability in the Deep Western Boundary Current: Local versus remote forcing. *Journal of Geophysical Research*, 117(C12), C12022. <https://doi.org/10.1029/2012JC008369>
- Petit, T., Lozier, M. S., Josey, S. A., & Cunningham, S. A. (2020). Atlantic deep water formation occurs primarily in the Iceland Basin and Irminger Sea by local buoyancy forcing. *Geophysical Research Letters*, 47(22), e2020GL091028. <https://doi.org/10.1029/2020GL091028>
- Pickart, R. S., & Spall, M. A. (2007). Impact of Labrador Sea convection on the North Atlantic Meridional Overturning Circulation. *Journal of Physical Oceanography*, 37(9), 2207–2227. <https://doi.org/10.1175/JPO3178.1>
- Pickart, R. S., Straneo, F., & Moore, G. W. K. (2003). Is Labrador Sea Water formed in the Irminger Basin? *Deep Sea Research Part I: Oceanographic Research Papers*, 50(1), 23–52. [https://doi.org/10.1016/S0967-0637\(02\)00134-6](https://doi.org/10.1016/S0967-0637(02)00134-6)
- Rhein, M., Kieke, D., & Steinfeldt, R. (2007). Ventilation of the upper Labrador Sea Water, 2003–2005. *Geophysical Research Letters*, 34(6), L06603. <https://doi.org/10.1029/2006GL028540>
- Rieck, J. K., Böning, C. W., & Getzlaff, K. (2019). The nature of eddy kinetic energy in the Labrador Sea: Different types of mesoscale eddies, their temporal variability, and impact on deep convection. *Journal of Physical Oceanography*, 49(8), 2075–2094. <https://doi.org/10.1175/JPO-D-18-0243.1>
- Schmid, C. (2014). Mean vertical and horizontal structure of the subtropical circulation in the South Atlantic from three-dimensional observed velocity fields. *Deep Sea Research*, 91(9), 50–71. <https://doi.org/10.1016/j.dsr.2014.04.015>
- Schott, F. A., Stramma, L., Giese, B. S., & Zantopp, R. (2009). Labrador Sea convection and Subpolar North Atlantic Deep Water export in the SODA assimilation model. *Deep Sea Research Part I: Oceanographic Research Papers*, 56(6), 926–938. <https://doi.org/10.1016/j.dsr.2009.01.001>
- Schott, F. A., Zantopp, R., Stramma, L., Dengler, M., Fischer, J., & Wibaux, M. (2004). Circulation and deep-water export at the Western exit of the Subpolar North Atlantic. *Journal of Physical Oceanography*, 34(4), 817–843. [https://doi.org/10.1175/1520-0485\(2004\)034<0817:CADEAT>2.0.CO;2](https://doi.org/10.1175/1520-0485(2004)034<0817:CADEAT>2.0.CO;2)
- Smethie, W. M., Jr., Fine, R. A., Putzka, A., & Jones, E. P. (2000). Tracing the flow of North Atlantic Deep Water using chlorofluorocarbons. *Journal of Geophysical Research: Oceans*, 105(C6), 14297–14323. <https://doi.org/10.1029/1999JC000274>
- Spall, M. A. (1996a). Dynamics of the Gulf Stream/Deep Western Boundary Current crossover. Part I: Entrainment and recirculation. *Journal of Physical Oceanography*, 26(10), 2152–2168. [https://doi.org/10.1175/1520-0485\(1996\)026<2152:DOTGSW>2.0.CO;2](https://doi.org/10.1175/1520-0485(1996)026<2152:DOTGSW>2.0.CO;2)
- Spall, M. A. (1996b). Dynamics of the Gulf Stream/Deep Western Boundary Current crossover. Part II: Low-frequency internal oscillations. *Journal of Physical Oceanography*, 26(10), 2169–2182. [https://doi.org/10.1175/1520-0485\(1996\)026<2169:DOTGSW>2.0.CO;2](https://doi.org/10.1175/1520-0485(1996)026<2169:DOTGSW>2.0.CO;2)
- Stramma, L., Kieke, D., Rhein, M., Schott, F., Yashayaev, I., & Koltermann, K. P. (2004). Deep water changes at the western boundary of the Subpolar North Atlantic during 1996–2001. *Deep Sea Research Part I: Oceanographic Research Papers*, 51(8), 1033–1056. <https://doi.org/10.1016/j.dsr.2004.04.001>
- Straneo, F. (2006). Heat and freshwater transport through the central Labrador Sea. *Journal of Physical Oceanography*, 36(4), 606–628. <https://doi.org/10.1175/JPO2875.1>
- Straneo, F., Pickart, R. S., & Lavender, K. (2003). Spreading of Labrador Sea Water: An advective-diffusive study based on Lagrangian data. *Deep Sea Research Part I: Oceanographic Research Papers*, 50(6), 701–719. [https://doi.org/10.1016/S0967-0637\(03\)00057-8](https://doi.org/10.1016/S0967-0637(03)00057-8)
- Talley, L. D., & McCartney, M. S. (1982). Distribution and circulation of Labrador Sea Water. *Journal of Physical Oceanography*, 12(11), 1189–1205. [https://doi.org/10.1175/1520-0485\(1982\)012<1189:DACOLS>2.0.CO;2](https://doi.org/10.1175/1520-0485(1982)012<1189:DACOLS>2.0.CO;2)
- Toole, J. M., Curry, R. G., Joyce, T. M., McCartney, M., & Peña Molino, B. (2011). Transport of the North Atlantic Deep Western Boundary Current about 39°N, 70°W: 2004–2008. *Deep Sea Research Part II: Topical Studies in Oceanography*, 58(17–18), 1768–1780. <https://doi.org/10.1016/j.dsr2.2010.10.058>
- Våge, K., Pickart, R. S., Sarafanov, A., Knutsen, O., Mercier, H., Lherminier, P., et al. (2011). The Irminger Gyre: Circulation, convection, and interannual variability. *Deep Sea Research Part I: Oceanographic Research Papers*, 58(5), 590–614. <https://doi.org/10.1016/j.dsr.2011.03.001>
- van Aken, H. M. (2000). The hydrography of the mid-latitude Northeast Atlantic Ocean: II: The intermediate water masses. *Deep Sea Research Part I: Oceanographic Research Papers*, 47(5), 789–824. [https://doi.org/10.1016/S0967-0637\(99\)00112-0](https://doi.org/10.1016/S0967-0637(99)00112-0)
- van Aken, H. M., de Jong, M. F., & Yashayaev, I. (2011). Decadal and multi-decadal variability of Labrador Sea Water in the north-western North Atlantic Ocean derived from tracer distributions: Heat budget, ventilation, and advection. *Deep Sea Research Part I: Oceanographic Research Papers*, 58(5), 505–523. <https://doi.org/10.1016/j.dsr.2011.02.008>
- van Sebille, E., Baringer, M. O., Johns, W. E., Meinen, C. S., Beal, L. M., de Jong, M. F., & Aken, H. M. (2011). Propagation pathways of classical Labrador Sea water from its source region to 26°N. *Journal of Geophysical Research*, 116(C12), C12027. <https://doi.org/10.1029/2011JC007171>

- Yashayaev, I. (2007). Hydrographic changes in the Labrador Sea, 1960–2005. *Progress in Oceanography*, 73(3–4), 242–276. <https://doi.org/10.1016/j.pocean.2007.04.015>
- Yashayaev, I., Bersch, M., & van Aken, H. M. (2007). Spreading of the Labrador Sea Water to the Irminger and Iceland basins. *Geophysical Research Letters*, 34(10). <https://doi.org/10.1029/2006GL028999>
- Yashayaev, I., & Clarke, A. (2008). Evolution of North Atlantic water masses inferred from Labrador Sea salinity series. *Oceanography*, 21(1), 30–45. Retrieved from <https://www.jstor.org/stable/2486015210.5670/oceanog.2008.65>
- Yashayaev, I., & Loder, J. W. (2008). *Replenishment of Labrador Sea Water to the ocean conveyor belt in 2008* (Vol. 28). Bedford Institute of Oceanography.
- Yashayaev, I., & Loder, J. W. (2009). Enhanced production of Labrador Sea Water in 2008. *Geophysical Research Letters*, 36(1). <https://doi.org/10.1029/2008GL036162>
- Yashayaev, I., & Loder, J. W. (2016). Recurrent replenishment of Labrador Sea Water and associated decadal-scale variability. *Journal of Geophysical Research: Oceans*, 121(11), 8095–8114. <https://doi.org/10.1002/2016JC012046>
- Yashayaev, I., & Loder, J. W. (2017). Further intensification of deep convection in the Labrador Sea in 2016. *Geophysical Research Letters*, 44(3), 1429–1438. <https://doi.org/10.1002/2016GL071668>
- Yashayaev, I., Seidov, D., & Demirov, E. (2015). A new collective view of oceanography of the Arctic and North Atlantic basins. *Progress in Oceanography*, 132, 1–21. <https://doi.org/10.1016/j.pocean.2014.12.012>
- Yashayaev, I., van Aken, H. M., Holliday, N. P., & Bersch, M. (2007). Transformation of the Labrador Sea Water in the Subpolar North Atlantic. *Geophysical Research Letters*, 34(22). <https://doi.org/10.1029/2007GL031812>
- Zantopp, R., Fischer, J., Visbeck, M., & Karstensen, J. (2017). From interannual to decadal: Seventeen years of boundary current transports at the exit of the Labrador Sea. *Journal of Geophysical Research: Oceans*, 122(3), 1724–1748. <https://doi.org/10.1002/2016JC012271>
- Zhang, R., & Thomas, M. (2021). Horizontal circulation across density surfaces contributes substantially to the long-term mean northern Atlantic Meridional Overturning Circulation. *Communications Earth & Environment*, 2(1), 1–12. <https://doi.org/10.1038/s43247-021-00182-y>
- Zou, S., & Lozier, M. S. (2016). Breaking the linkage between Labrador Sea Water production and its export to the subtropical gyre. *Journal of Physical Oceanography*, 46(7), 2169–2182. <https://doi.org/10.1175/JPO-D-15-0210.1>